From Oblique Subduction to Intra-Continental Transpression: Structures of the Southern Kermadec-Hikurangi Margin from Multibeam Bathymetry, Side-Scan Sonar and Seismic Reflection

JEAN-YVES COLLOT[1,4], JEAN DELTEIL[2], KEITH B. LEWIS[3], BRYAN DAVY[4], GEOFFROY LAMARCHE[1,4], JEAN-CHRISTOPHE AUDRU[2] , PHIL BARNES[3], FRANCK CHANIER[5], ERIC CHAUMILLON[6], SERGE LALLEMAND[7], BERNARD MERCIER DE LEPINAY[2], ALAN ORPIN[8], BERNARD PELLETIER[9], MARC SOSSON[2], BERTRAND TOUSSAINT[1] and CHRIS URUSKI[4]

[1] *ORSTOM, B. P. 48, 06230 Villefranche s/mer, France*
[2] *Institut de Géodynamique, rue Albert Einstein 06560, Valbonne, Nice, France*
[3] *NIWA, P. O. Box 14901, Kilbirnie, Wellington, New Zealand*
[4] *IGNS, P. O. Box 1320, Wellington, New Zealand*
[5] *Laboratoire de Géologie Dynamique, Université des Sciences et Technologies de Lille 1, 59655, Villeneuve d 'Asq, France*
[6] *Laboratoire de Géodynamique sous-marine, B. P. 48, 06230, Villefranche s/mer, France*
[7] *Laboratoire de Géologie Structurale, Université de Montpellier II, Place Eugène Bataillon, 34095 Montpellier, France*
[8] *Department of Earth Sciences, James Cook University of North Queensland, Townsville, Q 4811, Australia*
[9] *ORSTOM, B. P. A5, Nouméa, Nouvelle-Calédonie*

(Received 10 April 1995; accepted 15 July 1995)

Key words: Oblique subduction, strike-slip faults, transpressive deformation, tectonic erosion, tectonic accretion, seamount collision, multibeam bathymetry

Abstract. The southern Kermadec-Hikurangi convergent margin, east of New Zealand, accommodates the oblique subduction of the oceanic Hikurangi Plateau at rates of 4–5 cm/yr. Swath bathymetry and sidescan data, together with seismic reflection and geopotential data obtained during the GEODYNZ-SUD cruise, showed major changes in tectonic style along the margin. The changes reflect the size and abundance of seamounts on the subducting plateau, the presence and thickness of trench-fill turbidites, and the change to increasing obliquity and intracontinental transpression towards the south. In this paper, we provide evidence that faulting with a significant strike-slip component is widespread along the entire 1000 km margin. Subduction of the northeastern scarp of the Hikurangi Plateau is marked by an offset in the Kermadec Trench and adjacent margin, and by a major NW-trending tear fault in the scarp. To the south, the southern Kermadec Trench is devoid of turbidite fill and the adjacent margin is characterized by an up to 1200 m high scarp that locally separates apparent clockwise rotated blocks on the upper slope from strike-slip faults and mass wasting on the lower slope. The northern Hikurangi Trough has at least 1 km of trench-fill but its adjacent margin is characterized by tectonic erosion. The toe of the margin is indented by 10–25 km for more than 200 km, and this is inferred to be the result of repeated impacts of the large seamounts that are abundant on the northern Hikurangi Plateau. The two most recent impacts have left major indentations in the margin. The central Hikurangi margin is characterized by development of a wide accretionary wedge on the lower slope, and by transpression of pre-subduction passive margin sediments on the upper slope. Shortening across the wedge together with a component of strike-slip motion on the upper slope supports an interpretation of some strain partitioning. The southern Hikurangi margin is a narrow, mainly compressive belt along a very oblique, apparently locked subduction zone.

Marine Geophysical Researches **18:** 357–381, 1996.

1. Introduction

Along the Pacific-Australian plate boundary, the obliquely convergent margin from the southern Kermadec Trench to the southern limit of the Hikurangi Trough off northern South Island, New Zealand provides an ideal setting to study structures associated with the transition from oblique intra-oceanic subduction to intra-continental transpression. The large-scale morphology and tectonics of this active margin have been defined by nearly three decades of geophysical reconnaissance (Houtz *et al.*, 1967; Karig, 1970; Katz, 1974; Lewis, 1980; Davey *et al.*, 1986; Gillies and Davey, 1986; Davy, 1992; Lewis and Pettinga, 1993). In November 1993, EM12Dual multibeam bathymetry, side-scan sonar imagery, 6 channel seismic reflection and geopotential data were acquired during the GEODYNZ-SUD cruise of the R/V *l'Atalante* over the southern Kermadec-Hikurangi margin and the adjacent Pacific plate (Collot *et al.*, 1995). Morphologically, the margin can be divided, from north to south, into a southern Kermadec, northern Hikurangi, central Hikurangi, and southern Hikurangi segments. All four segments of the margin are underthrust by the oceanic Hikurangi Plateau (Figures 1 and 2). The new data sets have refined complex sedimentologic and deformation patterns, and helped clarify how these patterns relate to kinematics, to the changing nature of the lithosphere on both plates, and to variations in trench fill sediment.

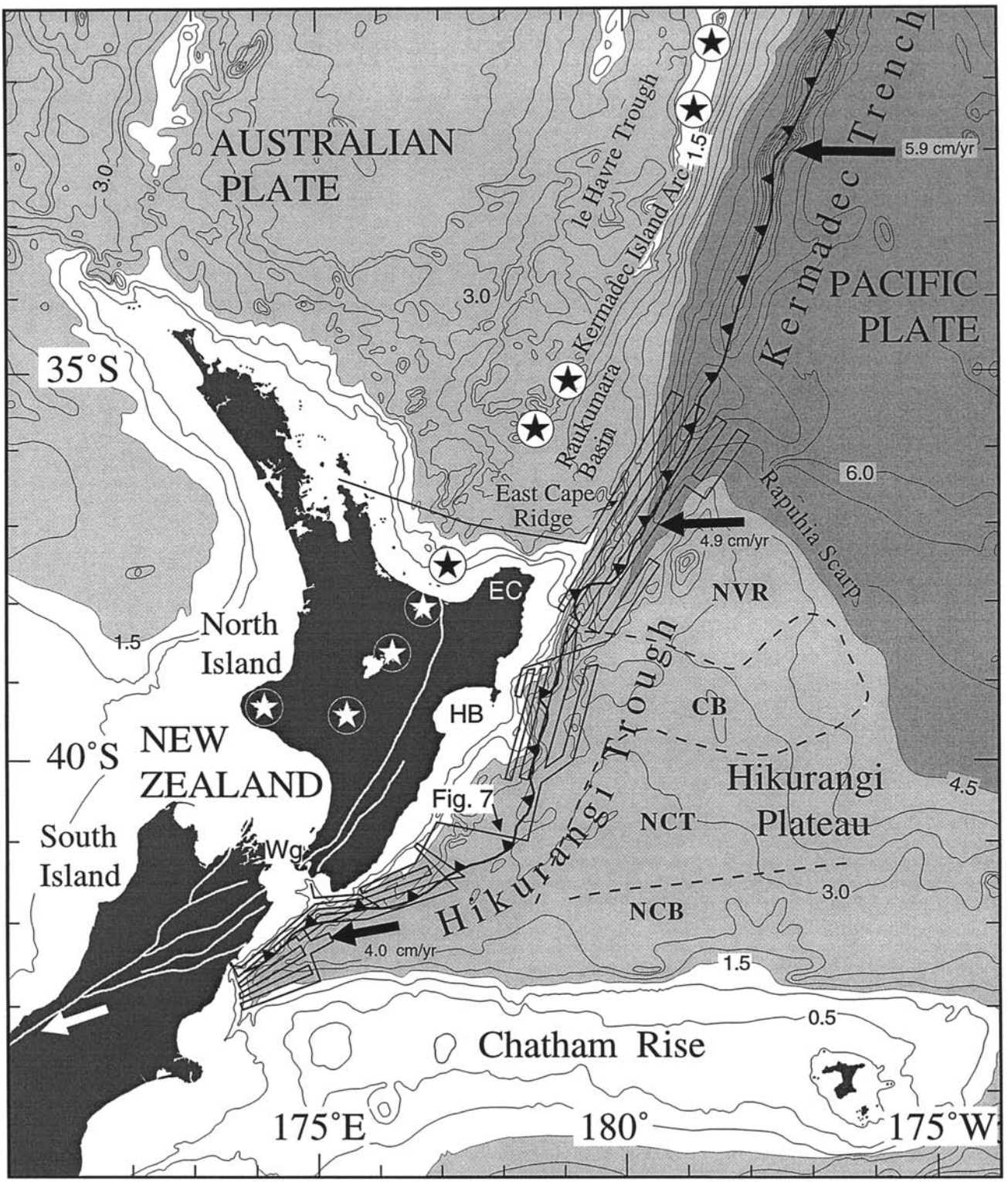

Fig. 1. New Zealand geodynamic setting with ship tracks of the GEODYNZ-SUD cruise; bathymetry is in km; 500 m contours; line with teeth is the deformation front; white lines are major onshore strike-slip faults; circled stars are major active volcanoes; arrows are PAC-AUS plate convergence direction from De Mets *et al.*, (1990); NVR: northern volcanic region; CB: central basin; NCT: northern Chatham terrace; NCB: northern Chatham basin; EC: East Cape; HB: Hawke Bay; Wg: Wellington.

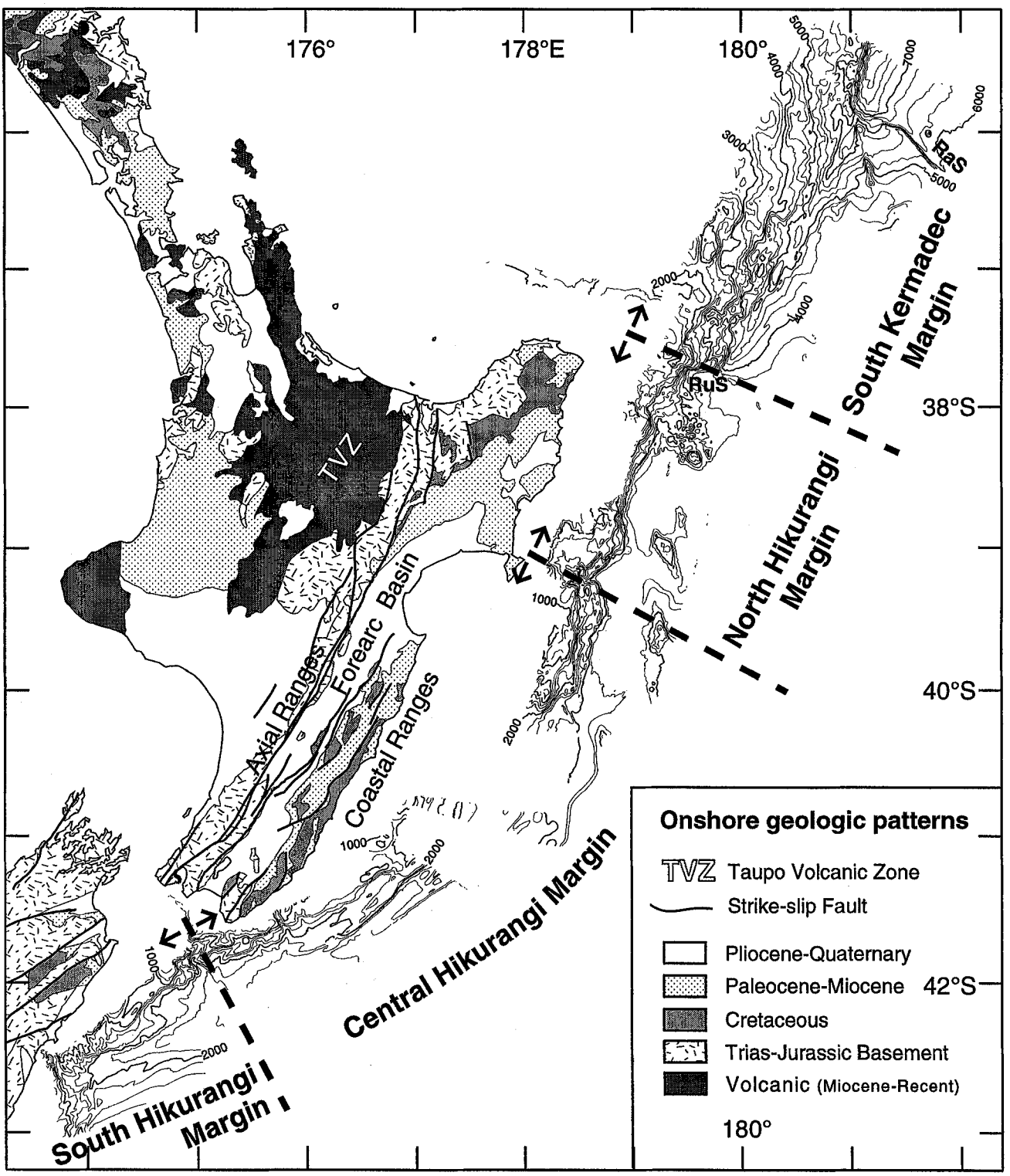

Fig. 2. Geologic map of New Zealand, with simplified multibeam bathymetry of the Southern Kermadec-Hikurangi margin; 250 m contours; the dashed lines and arrows separate the four structural segments of the margin; RaS: Rapuhia scarp; RuS: Ruatoria scarp.

2. Geological Setting of the Kermadec-Hikurangi Subduction Zone

North Island, New Zealand is located above a subduction zone at the southern limit of the Kermadec Trench-Hikurangi Trough plate boundary (Walcott, 1978a). The proximity of the PAC-AUS pole of rotation at 60.1° S, 178.3° E (De Mets *et al.*, 1990) for this plate boundary means that the direction and rate of convergence change rapidly along the margin. In the Kermadec Trench, at 37° S, the angle between the margin and the convergence direction is 60° and the rate of convergence is 4.9 cm/yr. At 42° S, they are 20° and 4.0 cm/yr. Therefore, subduction is progressively more oblique southward along the margin. Southwest of 42° S the subduction changes to intra-continental collision along the Alpine Fault, a major dextral-reverse fault (Wellman, 1953; Berryman *et al.*, 1992). Plate kinematic reconstructions indicate that subduction has become more orthogonal since about 5 Ma, reflected by the westward migration of the PAC/AUS rotation pole (summarized in Sutherland, 1995).

The oblique Kermadec-Hikurangi convergent plate boundary shows considerable structural and sedimentological variations along strike (Figure 1). North of 36° S, the oceanic Pacific plate is subducted westward beneath the oceanic lithosphere of the Kermadec volcanic arc and back-arc Havre Trough along the northern and central Kermadec Trench (Karig, 1970; Katz, 1974; Wright, 1993). Between 36° S and East Cape, an ocean-continent transitional margin is underthrust by the oceanic Hikurangi Plateau (Davy, 1992). Further south, the Hikurangi Plateau is subducted beneath the continental lithosphere of New Zealand (Walcott, 1978a; Katz, 1982; Davy, 1992; Lewis and Pettinga, 1993).

2.1. The Hikurangi Plateau

On the Pacific plate, the oceanic Hikurangi Plateau is a triangular area of elevated (3–4 km), 10–15 km-thick crust (Davy and Wood, 1994) bounded to the northeast by the 1 km-high Rapuhia Scarp and to the south by the Chatham Rise, which rises to less than 400 m. Basement on the plateau is interpreted as pre-Tertiary volcanic rocks overlain by 500–2000 m of sediment (Wood and Davy, 1994). MORB basalts dredged from the base of the Rapuhia Scarp are similar isotopically to those of the Cretaceous Ontong-Java and Manihiki plateaus (Mortimer and Parkinson, 1996).

Davy and Wood (1994) identified four morphologic and sedimentologic regions that abut the Kermadec-Hikurangi trench (Figure 1). From north to south these are:

1. The northern volcanic region, elevated by 500 m above the rest of the Plateau, is covered by less than 1 second of sediment.
2. The central basin, which is turbidite filled and contains 1–-1.6 seconds of sediment and the extension of the modern Hikurangi channel from the Hikurangi Trough (Lewis, 1994).
3. The northern Chatham terrace has a similar basement depth to that of the northern volcanic region but has 0.6 to 1.2 second of sediment cover.
4. The northern Chatham basin contains up to 2.5 seconds of sediment and overlies a south-dipping basement.

Volcanic peaks are wide-spread throughout the plateau but appear more extensive in its northern region. Large peaks are Cretaceous or older (Strong, 1994); smaller ones may have been emplaced in late Miocene to Recent times (Lewis and Bennett, 1985).

2.2. The Kermadec-Hikurangi Margin

The equivalents of the Kermadec Quaternary volcanic arc and its associated Plio-Pleistocene rifted back-arc Havre Trough extend southward into the continental crust of North Island 's Taupo Volcanic Zone (Karig, 1970; Smith *et al.*, 1989; Wright, 1993; 1994) (Figures 1 and 2). This extensional zone is intruded by Quaternary island arc andesite attesting to active subduction (Cole, 1990). However, subduction-related volcanism is known to have existed northwest of the Taupo Volcanic Zone since the early Miocene, indicating that a phase of subduction began beneath the northwestern North Island about 23–25 Ma ago (Ballance, 1976; Kamp, 1984; Spörli and Ballance, 1989; Herzer, 1995).

The southern Kermadec forearc comprises the triangular-shaped Raukumara forearc basin (Figure 1) bounded eastward by the East Cape Ridge that towers over a steep inner trench wall (Karig, 1970; Katz, 1974). The Raukumara forearc basin lies under 2400 m of water and contains more than 4 km of Cenozoic sediment overlying a gently eastward rising acoustic basement extending to the East Cape Ridge (Gillies and Davey, 1986).

In the North Island, the forearc region consists of a broad (up to 200 km) deforming zone that comprises two faulted ranges trending parallel to the volcanic arc and separated by a forearc basin (van der Lingen and Pettinga, 1980; van der Lingen, 1982) (Figure 2). The axial ranges form the western belt and are composed of Triassic and Jurassic greywacke presently deforming by uplift (Pillans, 1986) and dextral strike-

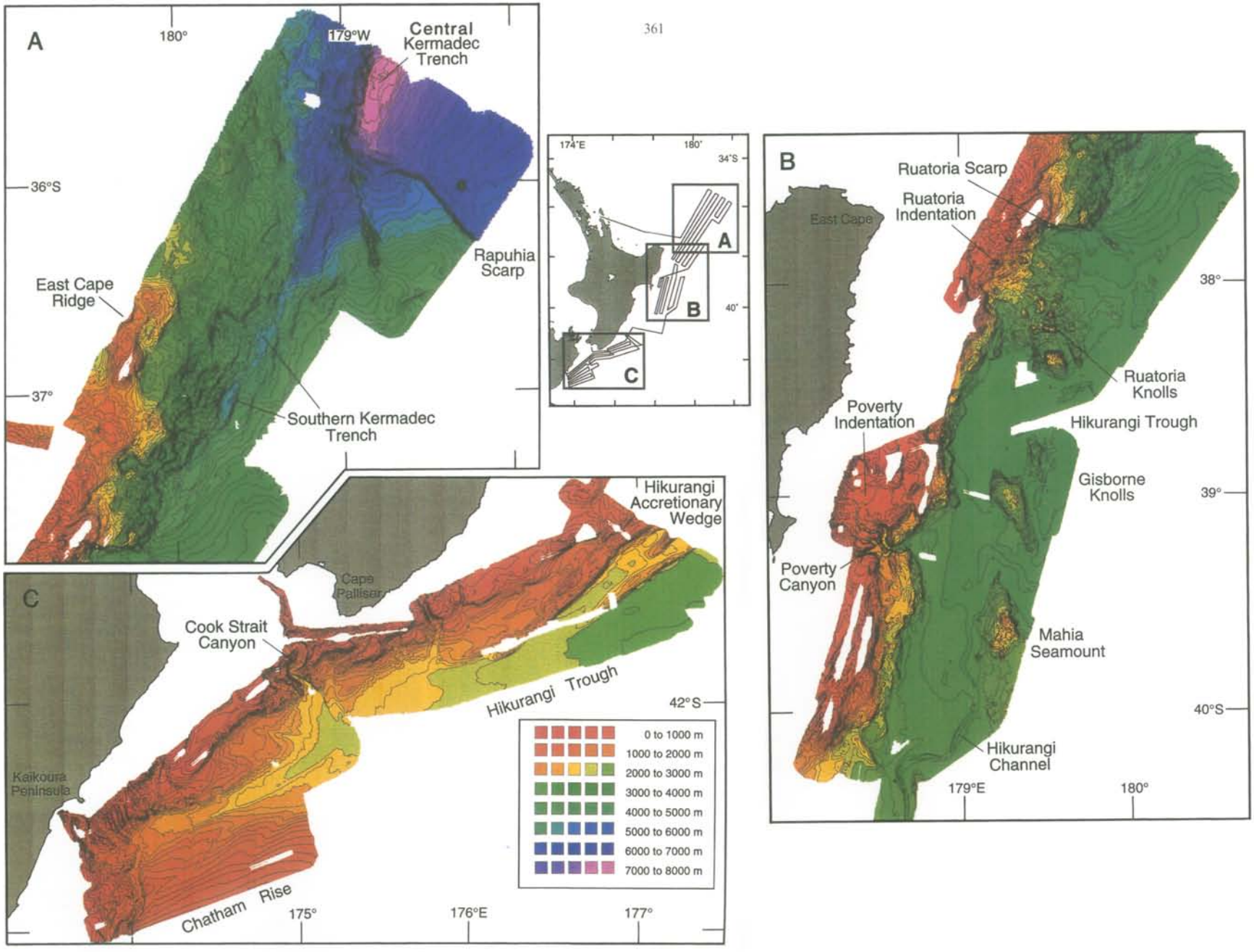

Fig. 3. Multibeam bathymetry of three areas of the Kermadec-Hikurangi margin with 100 m contours. Areas covered are shown on the central insert.

slip faulting (Berryman and Beanland, 1988; Cashman *et al.*, 1992). The forearc basin consists of sequences of Neogene marine and late Quaternary terrigenous deposits unconformably overlying Mesozoic greywacke or Upper Cretaceous to Paleogene rocks (Neef, 1984; Ballance, 1993). Since the latest Pliocene this basin has been deformed by reverse and dextral strike-slip faulting (Pettinga, 1982; Cashman *et al.*, 1992; Lamarche *et al.*, 1995; Kelsey *et al.*, 1995). The coastal ranges, which form the eastern belt, consist of Neogene flysch basins separated by complexly deformed Cretaceous to Oligocene ridges of the pre-subduction continental margin. Present day deformation of the coastal ranges includes folding, modest reverse faulting (van der Lingen and Pettinga, 1980; Pettinga, 1982; Chanier and Ferrière, 1991), strike-slip faulting (Cashman *et al*, 1992; Delteil *et al.*, in press) and normal faulting (Cashman and Kelsey, 1990).

Offshore of the North Island, the Hikurangi margin comprises an upper margin that consists of compressively-deformed Cretaceous and Cenozoic pre-subduction sediment (Lewis and Bennet, 1985) and a lower margin interpreted as imbricated Plio-Pleistocene and offscraped trench sediments forming the Hikurangi accretionary wedge (Lewis, 1980; Cole and Lewis, 1981, Davey *et al.*, 1986; Lewis and Pettinga, 1993). The upper margin, however, could involve strain-hardened accreted rocks from the initial stage of subduction. Neogene and Quaternary basins are developed on the upper margin and between the accretionary ridges (Lewis, 1980).

The latitudinal segmentation of the Hikurangi margin has long been recognized on the basis of its morphologic and seismic characters (Katz, 1974, 1982; Katz and Wood, 1980). Southern, central and northern structural segments were identified by Lewis and Pettinga (1993). The southern segment, south of Cook Strait, has a steep, continental margin with minimal offscraped trench-fill. The central segment between Cook Strait and Hawke Bay has a gentle slope and comprises most of the large Plio-Pleistocene accretionary wedge. The northern segment shows a steep slope and little evidence for accreted trench fill (Lewis and Pettinga, 1993).

The distribution of earthquake epicenters beneath the North Island defines a shallow (10°–20°) northwest dipping Benioff zone extending 200 km westward from the trench. Past that location, the dip steepens to 60°–70° between depths of 80 and 300 km (Reyners, 1989). The Benioff zone becomes nearly vertical beneath Wellington and northern South Island (Anderson and Webb, 1994).

3. Geophysical Data

The EM12Dual from SIMRAD™ is a hull-mounted mapping system that collects bathymetric and sonar backscatter data in swaths up to 22 km wide. One EM12 unit is mounted on the port side and one on the starboard side. Each generates 81 stabilized beams at frequencies of 12.6 to 13 kHz providing 162 simultaneous soundings using both phase and energy measurement of the backscattered signal. The survey was done at 10 knots and covered 80,000 km^2 in 18 days. Tracks were oriented parallel to the dominant structural trends in order to optimize the side scan imaging characteristics of the EM12D, although this orientation is not ideal for seismic reflection data. The 6-channel seismic reflection data were shot with two 75 cu in, SODERA™ GI guns. Magnetic data were acquired at 6-seconds sampling interval using a BARRINGER M-244 proton magnetometer and gravity data were collected using a BODENSEEWERK KSS30 gravitymeter. During the cruise, the gravity data were automatically corrected for spring tension, cross coupling, Eötvos, and for latitude according to the International Gravity Standardization Network 1971 ellipsoid.

4. Morphology and Shallow Structures of the Downgoing Plate

A 50 km-wide strip of the downgoing plate adjacent to the Kermadec-Hikurangi margin was surveyed. In this section we summarize, from north to south, the structures mapped along this strip including those of the Kermadec Trench and Hikurangi Trough.

The oceanic abyssal plain and underlying sediment immediately north of the Rapuhia Scarp smoothly bend northwestward from a depth of 6000 m into the 15 km-wide, flat-bottomed, 7800 m deep Kermadec Trench (Figure 3A). In the trench, imagery (Figure 4) and seismic reflection data indicate that the seafloor and sediment are disrupted by two sinuous, west facing normal faults that trend N–S and N17° E, slightly oblique to the N10° E trending trench. Seismic reflection data reveal that in the vicinity of the trench, the upper part of the Pacific plate comprises a 400–600 m-thick, bedded sedimentary sequence overlying a strongly reflective and stratified acoustic basement offset by faults. The upper sequence, which thins northward and shows internal erosional surfaces (Davy, 1992) is part of a fan-drift formed by interaction between the Deep Western Boundary Current (DWBC) and sediment transported along the Hikurangi Chan-

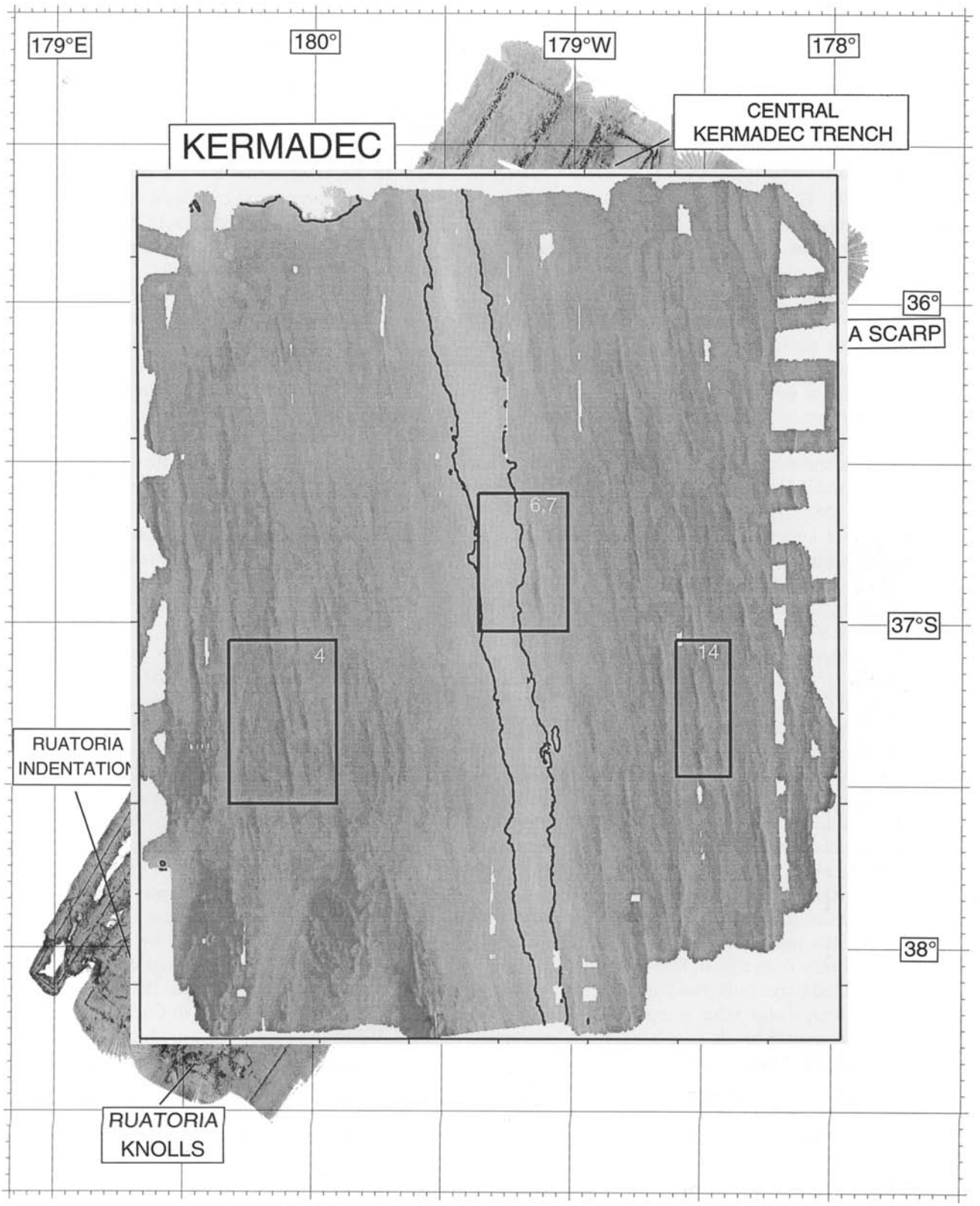

Fig. 4. Side scan sonar imagery of the southern Kermadec margin and Ruatoria indentation. Note the high reflectivity (black) of the Rapuhia Scarp, Ridges R1, R2 and R3 and the complex seafloor reflectivity of the Ruatoria indentation.

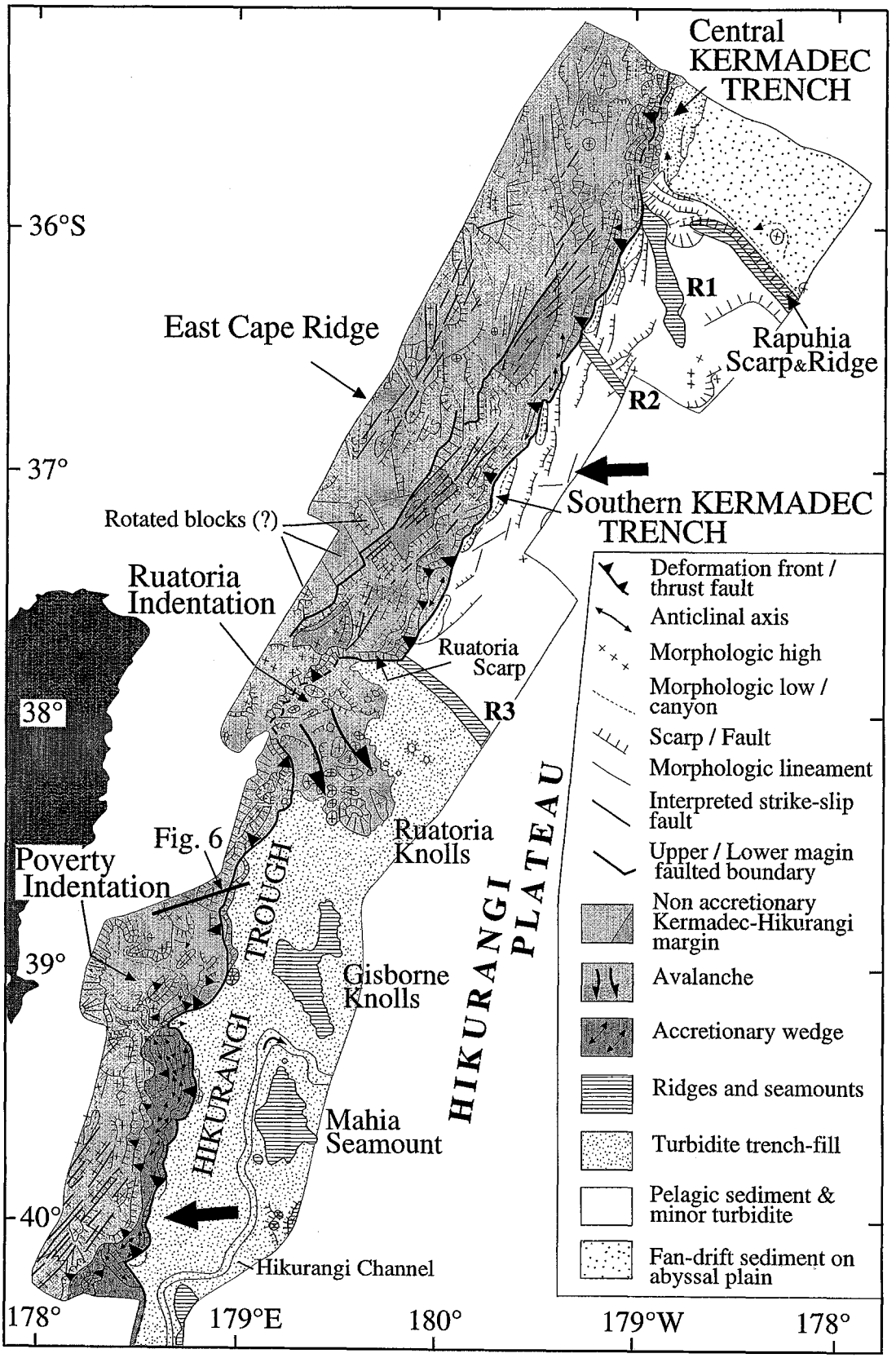

Fig. 5. Structural interpretation of the Kermadec-Hikurangi margin from 35° S to 40°10′ S; large arrows: plate convergence direction.

nel (Carter and McCave, 1994; Lewis, 1994). Scouring of the seafloor adjacent to the Rapuhia Scarp by the DWBC (Carter and McCave, 1994) has left a 7 km-wide, 150 m deep linear moat. The moat deepens northwestward (Lewis, 1994) and connects with the trench, indicating that it is a major conduit transporting remobilized fan-drift sediment into the central Kermadec trench (Figure 5). In the trench, up to 250 m of nearly horizontal, re-deposited turbidites unconformably overlie sediments of the downgoing plate.

The Rapuhia Scarp in the survey area is 1000 m-high, trends N140° E and dips 20° toward the northeast. Near its junction with the trench, the scarp changes trend to N110° E and breaks into three smaller scarps whose cumulate relief is about 1400 m. Geophysical data collected by *l'Atalante* combined with other surveys (Wood and Davy, 1994) indicate that the Rapuhia Scarp is formed by a magnetic ridge (200–500 nT), which underlies the northern edge of the Plateau (Figure 5).

The southern Kermadec Trench extends from the Rapuhia Scarp to 37°40′ S, trends N 28° E and shoals southward from 6400 m to 4500 m (Figure 3A). This trench is at least 1400 m shallower than the central Kermadec Trench. On the Hikurangi Plateau, the outer trench wall is cut by west-facing scarps that average 25 km in length and trend N 0°–20° E, oblique to the trench. Secondary scarps trend N 45°–60° E and are less than 10 km long. Both sets of scarps are interpreted as normal faults related to the bending of the plate. In the trench, the two cross-cutting sets of faults delineate seven right-stepping, structural troughs that are almost bare of sediment fill (Figure 5).

The section of the Hikurangi Plateau adjacent to the southern Kermadec Trench shallows from 5500 m in the north to 3700 m near 37°40′ S, a regional dip of 0.4°. The surface of the plateau is elevated at three ridges which obliquely intersect the trench. The three ridges have a strongly reflective surface (Figure 4) indicating that they are bare of recent sediment. The major ridge (R1), in the northern part of the plateau, is 1000 m high, trends N168° E and looks like a series of elongated volcanoes (Figure 3A). The second ridge (R2), at 36°35′ S, trends N140° E and has a subdued bathymetric expression. The third ridge (R3) at 37°40′ S trends N130°–150° E and is almost buried by sediment. Only the southern ridge is associated with moderately high (120–150 nT) magnetic anomalies supporting the interpretation of a volcanic origin. The third ridge acts as a barrier to northward turbidite transport from the Hikurangi Trough (Figure 5).

Swath coverage of the Hikurangi Trough between 37°40′ S and 40°20′ S has enabled recognition of the detailed morphology and seafloor texture of three areas of knolls and seamounts: the Ruatoria Knolls, the Gisborne Knolls and the Mahia Seamounts (Figure 3B). The Ruatoria Knolls consist of a series of about twelve elliptical to elongated mounds up to 1250 m high and roughly oriented NNW. Some mounds associated with moderate magnetic anomalies could be volcanic, whereas others may be slump blocks derived from the forearc. The Gisborne Knolls trend N155° E and N170° E (Figure 3B). The major knoll is 1000 m high and is bounded by steep linear scarps trending N 5° E, N110° E, N140° E and N170° E. Its flatish summit is topped by 200 m-high cones. Mahia Seamount is separated from the Gisborne Knolls by the meandering Hikurangi Channel. The seamount is 1250 m high, trends NNW and shows a chaotic summit morphology with numerous 100–300 m peaks. This seamount is delineated by structures trending N 20° E, N 35° E, N145° E and N165° E. The massive and rhomboidal shape of the Gisborne Knolls and Mahia Seamount, together with their strong magnetic anomalies (maximum amplitude +450 nT) suggest volcanic rocks emplaced at the intersection of major faults. A similar N140° E-oriented ridge impinging on the accretionary wedge at 40°12′ S (Figure 3B) shows only folded sedimentary structure with no associated magnetic anomaly. This ridge is probably not volcanic but rather is caused by deformation along a fault in the subducting basement.

The segment of the downgoing plate imaged from 40°30′ S to 42° S is the turbidite filled Hikurangi Trough with the 100 m deep, leveed Hikurangi channel meandering along it. This channel is inferred to be the conduit of sand-laden turbidity currents derived mainly from near the Kaikoura Peninsula (Figure 3C) (Lewis, 1994).

The northern flank of the Chatham Rise, in the southernmost part of the survey area, has a regular smooth slope with two wide, elongated depressions 250 m below the surrounding seafloor and trending N 50° E, oblique to the slope (Figure 3C). These depressions are strongly reflective and are inferred to be scours formed by currents during glacial ages (Barnes, 1994). The northwestern edge of the rise is marked by the 12 km-wide, N 60° E-trending, flat bottomed Hikurangi Channel.

5. Shallow Structures of the Over-Riding Plate: The Southern Kermadec-Hikurangi Margin

In the next section, we will describe from north to south the morphology and shallow structures of the

four segments of the Kermadec-Hikurangi margin (Figure 2):

1. The linear southern Kermadec segment between 35°10′ S and 37°45′ S.
2. The steep and indented northern Hikurangi segment between 37°45′ S and 39°15′ S that encompasses the Ruatoria and Poverty indentations.
3. The arcuate central Hikurangi segment that includes the Hikurangi accretionary wedge between 39°15′ S and 42° S.
4. The steep and narrow south Hikurangi segment between 42°–42° 30′ S.

5.1. The southern Kermadec segment

This segment of the Kermadec margin trends N28° E and terminates in the south at the Ruatoria Scarp, a major tectonic feature that cuts across the margin (Figures 2 and 3A). This boundary is coincident with the end of the Kermadec Trench and the half-buried ridge R3 on the plateau. The inner trench wall shallows from near 6000 m north of 36° S to 1000 m near 37°45′ S with an average dip of 0.9° that is twice the dip of the adjacent Plateau. Part of the along strike inner trench wall dip may be attributable to the SSW shoal of the Hikurangi Plateau suggesting differential uplift of the margin in response to the Plateau subduction. The remainder of the trench wall dip may reflect the crustal thickening of the upper plate, which likely accompanies the change from oceanic type crust in the north to continental in the south.

Morphology also changes greatly both along and across the strike of the margin. Based on morphologic variations, we divided this segment of the margin into a relatively smooth and gently (1–2°) seaward-dipping half north of 36°30′ S, and a rough, steeper eastward-dipping southern half.

5.1.1. The northern half

In the northern half, the gentle trenchward slope of the southern Kermadec margin is dominated by a large scale (20–50 km), roughly N170° E to NS trending, right-stepping structural grain combined with a subsidiary N 40° E grain (Figure 5). The N170° E grain is characterized by small east-facing scarps separating thinly sedimented terraces, slope basins and small ridges.

The lower part of this slope and the toe of the margin show considerable variation north and south of the Rapuhia Scarp-trench junction. North of the junction, the 8 km-wide toe of the margin is composed of steep (10°) braided scarps bounding small (1–5 km wide) lens-shaped terraces indicating a collapsing tectonic front. The southern limit of the terraces is coincident with rapid northward deepening of the southern Kermadec Trench across the 1.4 km-high Rapuhia Scarp. At the scarp-trench junction, a small N170° E trending bulge deforms the lower slope and is aligned with ridge R1 of the Hikurangi Plateau, suggesting that the bulge results from the subduction of the northward extension of ridge R1. Immediately south of the junction, scarps and a narrow ridge trending N15° E parallel the major set of normal faults of the Hikurangi Plateau and indicate that the lower slope is structurally controlled by the subducted northwestern edge of the plateau.

5.1.2. The southern half

The southern half of the southern Kermadec margin divides along a major, N 35° E trending, zigzag scarp into a stepped upper margin with the high relief East Cape Ridge, and a lower margin that has a rough morphology and terminates sharply at 37°45′ S against the Ruatoria Scarp. The major N 35° E-trending scarp is a 150 km-long relay of locally left-stepped, 100-1200 m high, steep (12°–17°) scarp segments that trend N50° E and N15° E to N150° E.

The upper margin shows several structural trends. The N170° E to NS trending grain, although less pronounced than in the northern half of the survey, is still marked by 800 m-high slopes and scarps that flank the East Cape Ridge highs. These highs are also separated from adjacent slope basins by NNE striking scarps. Structural lineations trending N 30° E slice the East Cape Ridge summit along its length. These lineations sharply offset the bathymetric contours both vertically and horizontally, suggesting active faults with a possible strike-slip component. South of 37° S, the N170° E to NS trending grain is replaced by N150° E-striking slopes bounding discrete blocks that are 20 km wide by 25 km long (Figure 5). Apparent left offsets of their N 50° E trending, southeastern borders suggest that the blocks rotated clockwise about a vertical axis.

The lower margin shows three structural highs (darker area of margin, Figure 5) separated along strike by deep troughs and is deformed by a small-scale (5–10 km), strongly NNE-oriented linear grain. The structural highs are in fault contact with the upper margin along the major N 35° E trending scarp. Steep N150° E trending scarps cut transversely through the lower margin and define, in conjunction with segments of the dominant N 35° E trending scarp, the narrow reentrant at 36°40′ S and the deep trough at 37°20′ S (Figure 3A).

The NNE-trending morphologic grain that dominates the lower margin between 36°30′ S and 37°45′ S

consists of sets of N 30° to N 45° E trending lineaments that are straight and locally gently sinuous in plan view. Detailed ridge and scarp morphology together with the merger to the southwest of the lineaments with the major N 35° E trending scarp indicate a strike-slip component of faulting. The interpreted strike-slip faults are recognized along the lower margin as far north as 36°20′ S.

Complex structures that arise from collapse, strike-slip deformation and compression shape the toe of this half of the margin. Southeast facing, small (10–15 km) arcuate re-entrants suggesting slump scars together with linear scarps parallel to the interpreted strike-slip faults suggest that collapse and mass wasting affect the toe of the margin. However, minor arcuate ridges forming the tectonic front may result from localized tectonic accretion.

5.2. The northern Hikurangi segment

The northern Hikurangi segment trends N15° E and extends from Ruatoria Scarp to the southern edge of the Poverty indentation (Figure 3B). The toe of this segment of the margin forms a 200 km-long reentrant, 10 to 25 km landward of the margins to the north and south. This reentrant suggests that most of the lower margin described north of Ruatoria Scarp is missing along the northern Hikurangi margin (Figure 5).

At 38° S, the margin is incised by the 50 km-wide Ruatoria indentation, bounded on the north and south by steep walls. The Ruatoria Scarp forms the northern wall, a sub-linear 100–1400 m-high scarp. The southern wall consists of two major arcuate, 400–1500 m-high, scarps. The lower part of the indentation is floored by a roughly N170° E elongated mass with a highly chaotic topography, suggesting allochthonous rocks derived from a collapse of the margin. Because this indentation has steep walls (22°) that cut the lower margin to the depth of the trench, and because the northern wall trends sub-parallel to the plate convergence direction, we believe that the indentation and subsequent collapse occurred in the wake of a subducted seamount.

Between the Ruatoria indentation and the Poverty Canyon, the lower part of the margin is steep (10°) and shows small flat terraces at the top of steep scarps. The toe of the margin shows small lobate and elongated features that are interpreted from morphologic and seismic data to be caused by collapse and slumping. Seismic line GNZ 14 (Figure 6) extends across the Hikurangi Trough and margin. This line shows three slope basins overlying complexly-deformed and tilted blocks. The pattern of faulting and morphology indicate that, at some stage, the margin deformed by extension. The arched-shape and fault pattern of the block between the middle and lower basins suggests, however, that compression or transpression also deformed the margin. Seismic line GNZ 14 also shows that the Hikurangi Trough contains 0.7 seconds of poorly-reflective rocks overlying a strongly reflective unit. This unit can be traced westward for about 30 km beneath the margin, where the unit forms a bump. This bump, which cannot be entirely attributed to a pull up effect, is interpreted as part of a subducting seamount. The complex 200 nT magnetic anomaly over the lower part of the margin (Figure 6) could be due to a buried seamount complex.

The Poverty indentation that was interpreted by Lewis and Pettinga (1993) as a seamount scar is now recognized as a double feature consisting of lower and upper indentations (Figuers 3B and 5). The lower indentation coincides with the mouth of the Poverty canyon and is therefore connected to the Hikurangi Trough. This indentation is steep-sided. It has a "V" shape in plan view and deflects the tectonic front landward from N15° E to N 50° E suggesting that the lower indentation resulted from the subduction of a seamount. The upper indentation is the 35 km-wide Poverty indentation that lies under 1000–1500 m of water. It is sharply bounded upslope by a linear, N 20° E-trending, 500–600 m high scarp and on its northern and southern flanks by smooth and lobate slopes. This morphology implies that the margin subsided eastward along the N20° E trending scarp. Seismic reflection data indicate that the upper indentation contains at least 500–800 m of stratified sediment deeply incised by the Poverty canyon network. In addition to the evidence for subsidence, the seaward edge of this indentation is bounded by two N 30°–40° E trending short anticlines, which suggest that at some stage the margin deformed by compression or transpression.

In conclusion, the Northern Hikurangi margin appears to have undergone a complex tectonic evolution related to multiple seamount collisions. We interpret this evolution as consisting of a series of compressional and extensional events accompanied by slumping and eventually major gravitational collapse. These processes finally led to the destruction of almost the entire lower margin by tectonic erosion.

5.3. The central Hikurangi segment

Data collected during the GEODYNZ-SUD cruise show that the central Hikurangi margin, characterized by the Hikurangi accretionary wedge, extends from the Poverty canyon in the north to the Cook Strait

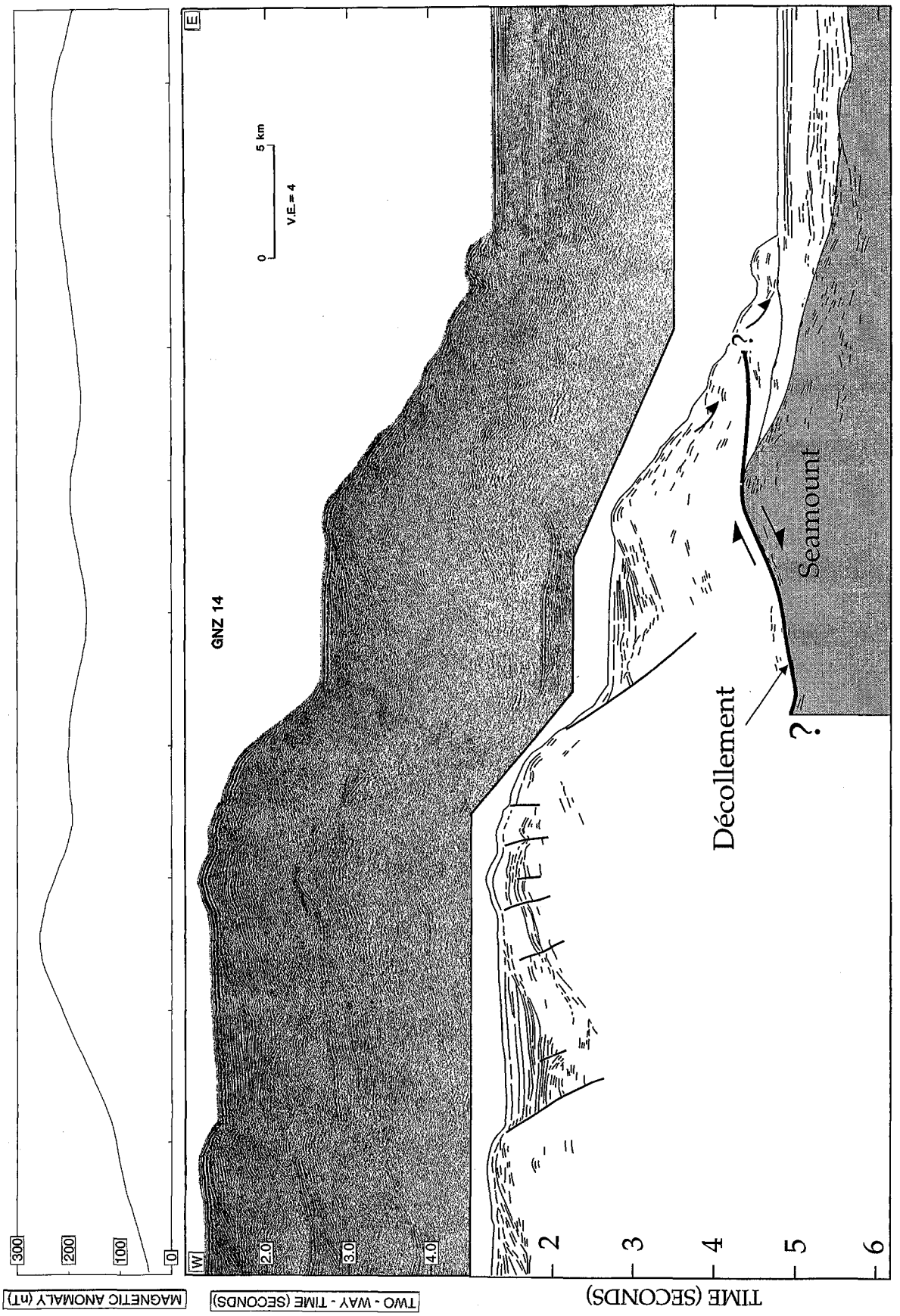

Fig. 6. Seismic reflection line GNZ 14, with magnetic anomaly and line drawing; location of line is shown in Figure 5; processing includes filtering, deconvolution, 3-fold stack, and migration with water velocity.

canyon in the south (Figure 2). The structural trend of this segment of the margin changes from N 15° E in the north to N 50° E and N 70° E in the south. These data allow us to refine the boundaries and structural styles of the pre-subduction upper margin and Plio-Pleistocene accretionary lower margin recognized by Lewis and Pettinga (1993).

Between 39°15′ S and 40°10′ S, upper and lower margins have distinct morphologies and structural trends (Figure 3B). The lower margin varies in width and depth along strike. It is 20 km wide at 2200 to 3250 m depth immediately south of the Poverty canyon but narrows to only 3 km at 2700–3000 m near 40° S (Figure 5). The lower margin has a low relief and consists of a series of linear to gently-curved ridges and flat-floored terraces. The ridges are asymmetric with a steeper and higher east flank. They generally parallel the N 15° E-trending margin except where they trend N 160° E at the southern edge of the Poverty canyon. Seismic profiles that cut across the ridges and terraces clearly image thrust faulting and growing anticlines of reflective and parallel-bedded sediment. These structures indicate that the lower margin is a recent imbricated fold and thrust belt that represents the northernmost extension of the Hikurangi accretionary wedge.

The upper margin has several massive, rounded and shallow (300–900 m) banks whose internal structures do not produce coherent reflections on seismic records. The southwestern part of the banks is dominated by a dense network of narrow ridges, valleys and linear, steep scarps trending N 35°–40° E, oblique to the banks (Figures 3B and 5). This morphology suggests that some of the scarps are formed by faults that slice an older topography. The faults and ridges trend 45° from the predicted plate convergence direction and probably result from transpressive deformation. The shape of the toe of the upper margin supports this interpretation. This toe has a zigzag trace in plan view, which may outline the northeast termination of upper margin strike-slip strips.

During the GEODYNZ-SUD cruise, we collected one swath traverse across the widest part of the accretionary wedge, near 41° S (Figure 7). This traverse indicates a change in slope angle and morphology near the depth of 2000 m. The upper margin consists of steep-sided, round-topped banks, and it has an average slope of 2.5°. The lower margin is 90 km-wide and has an average slope of 0.6°. It consists of a series of ridges and flat terraces that coincide with the anticlines and piggy-back basins of the accretionary wedge (Lewis, 1980; Davey *et al.*, 1986). Swath data show that some accreted ridges are discontinuous along strike and that the major ridges down slope become progressively more parallel to the trench. However, the deformation front, which trends N 05° E, locally deviates from the general trend of the wedge because of the collision of small seamounts. The gradual downslope change in strike of the accreted ridges may indicate a variation of the stress field orientation through time. Alternatively the Cenozoic upper margin may have controlled the orientation of the early accreted ridges, whereas the younger ridges further east developed independently of the older margin.

At the southern termination of the central Hikurangi margin (41° S–42° S) the boundary between the massive upper margin and accretionary lower margin is at depths of 1500 to 2000 m. In plan view, the accretionary wedge forms a corner that tapers southwestward (Figures 3C and 8). This wedge comprises upper and lower right-stepping accreting ridges trending N 50°-55° E and associated piggy-back basins. The deformation front follows the steep eastern flank of the extremely linear lower ridge and discontinuously steps to the right toward the mouth of the Cook Strait canyon. The accretionary wedge terminates at a short, ENE elongated anticline (Figure 8).

The upper margin diverges westward away from the axis of the accretionary ridges. Seismic reflection data indicate that thrust faults and folds deform the upper margin (Lewis and Pettinga, 1993). However, morphologic and new seismic reflection evidence discussed below indicates that the upper margin is also affected by some strike-slip motion leading to dextral transpressive deformation.

a) The edge of the upper margin shows a series of braided, steep scarps and structural lineaments that trend N 45°-N 60° E, sub-parallel to the margin, and converge across the Cook Strait canyon to form a horsetail tectonic pattern. Immediately east of Cook Strait the lineaments trend N 70° E, subparallel to the plate convergence vector, and delineate ENE-elongated structural blocks (darker grey, Figure 8) that may have been displaced laterally along faults. Northeast of these blocks, zigzag canyons appear horizontally offset by faults. EW-trending lineaments cut obliquely across the upper margin and are compatible with strike-slip faulting arising from oblique convergence. Those east of Cook Strait could be branches of the Kaikoura ranges transpressional faults that deform the northeastern South Island.
b) A small elongate high of the segment of the upper accretionary ridge adjacent to the upper margin (near 41°20′ S) appears to have been displaced along a morphologic lineament creating a comple-

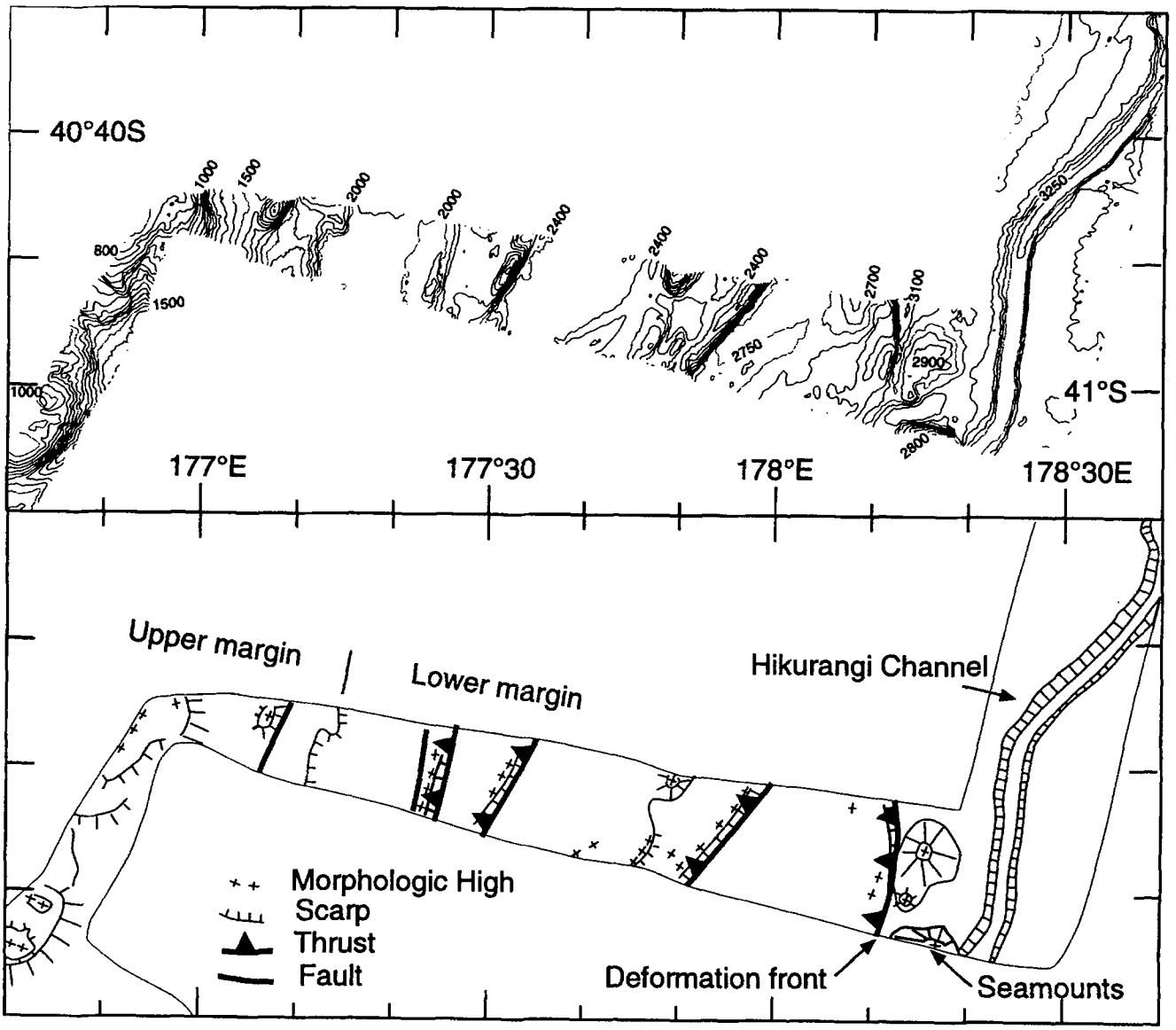

Fig. 7. Top: Multibeam bathymetric traverse across the Hikurangi accretionary wedge, 50 m contours; bottom: structural interpretation; location in Figure 1.

mentary low in its wake. This morphology suggests dextral strike-slip deformation along a N 45° E trending fault zone (Figure 9).

c) A flower structure is interpreted from seismic reflection line GNZ 36 (Figure 10) across the NE-trending region of this fault zone. This flower structure is indicated by a set of branching, high-angle faults that verge to both west and east. These faults deform a slope sedimentary basin, including its seafloor, attesting to their recent activity. Although the landward side of the basin has been predominantly controlled by differential subsidence, a sub-vertical fault zone associated with a localized compressive zone in the middle of the basin also suggests active transpressive deformation.

5.4. The southern Hikurangi segment

The southern segment of the margin extends from Cook Strait canyon to the Kaikoura Peninsula in the northeastern South Island (Figure 3C). This segment of the margin marks the beginning of the transition between subduction at the Hikurangi Trough and intra-continental transpression in the northern South Island.

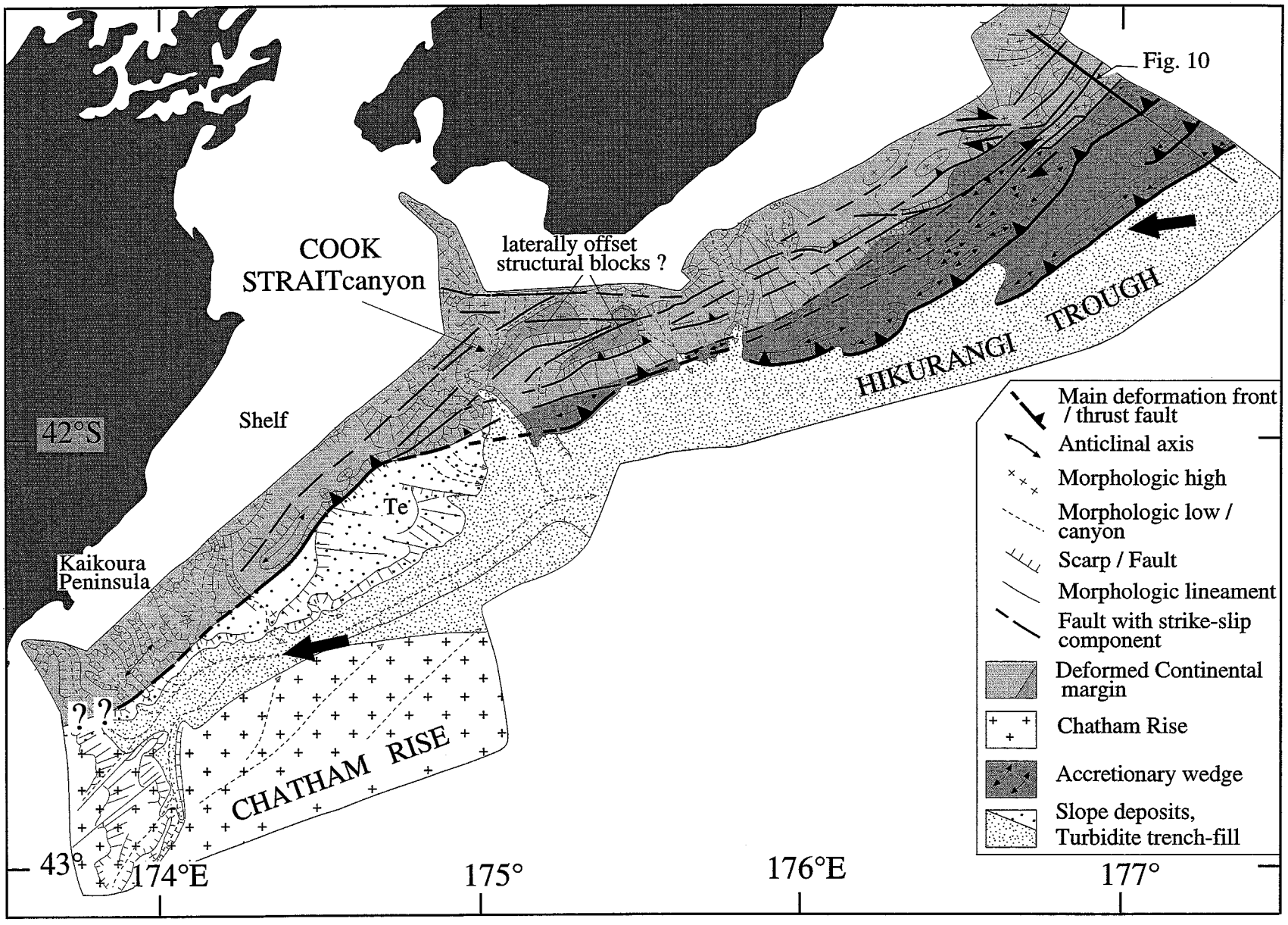

Fig. 8. Structural interpretation of central and southern Hikurangi margin; Te: lower terrace; large arrows: plate convergence direction.

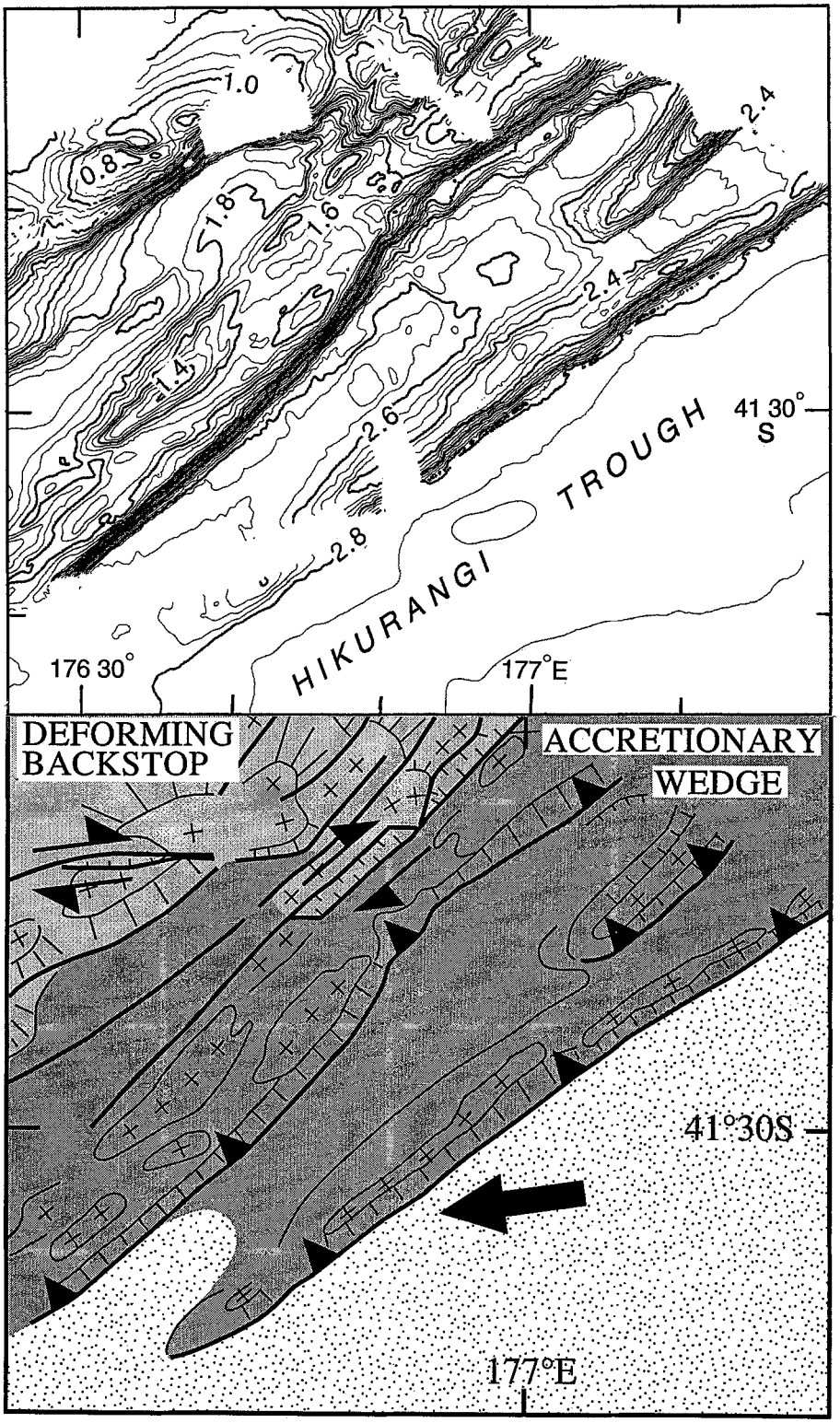

Fig. 9. Detailed multibeam bathymetry of the central Hikurangi margin showing evidence for transpressional deformation along the boundary between the Plio-Pleistocene accretionary wedge and the upper margin deforming back-stop; 50 m contours; symbols as in Figure 8.

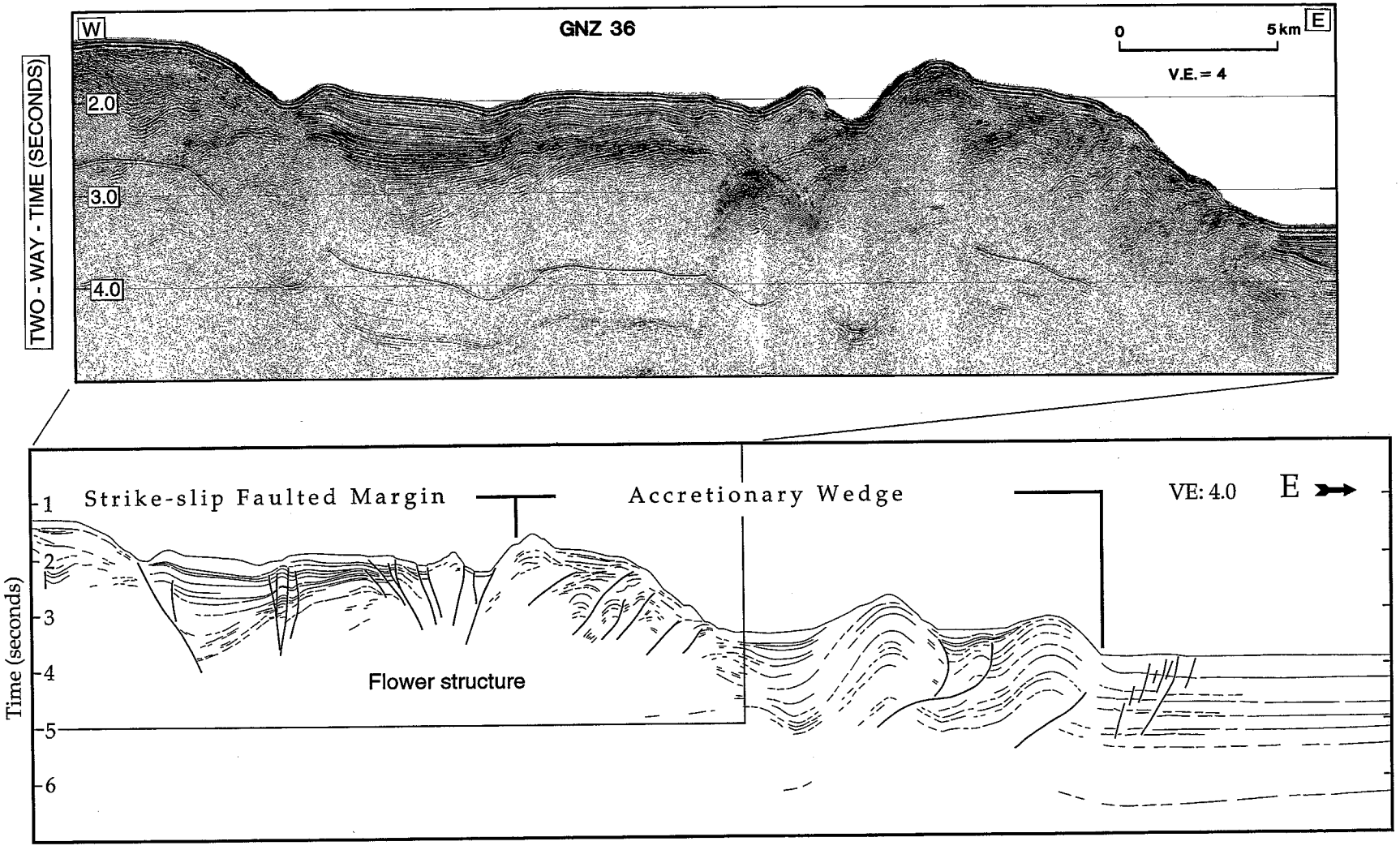

Fig. 10. Seismic reflection line GNZ 36, across the central Hikurangi margin. Seismic data in blow up show evidence for a flower structure within the upper margin; location of the line is shown in Figure 8; processing as for Figure 6.

The margin slope strikes N 45° E, is narrow and shows drastic changes in morphology along strike. An area of smooth seafloor without canyons separates the highly incised seafloor of the Cook Strait canyon from that of the southwestern end of the margin, which is also heavily incised.

The structure of the south Hikurangi margin differs greatly from that of the Hikurangi accretionary wedge, indicating that a classical imbricated accretionary wedge did not develop southwest of Cook Strait canyon. In the area of smooth seafloor, the margin divides into a weakly deformed lower slope terrace and a deformed upper slope comprising a 25 km by 8 km, 1000 m-deep perched basin and a prominent ridge (Figure 8). The basin contains 0.5–1 second of faulted sediments overlying a complexly-deformed acoustic basement that we interpret as rocks of the continental margin. The ridge trends N 45° E and is interpreted from seismic data as an anticline. Its steep southeastern flank has been identified as the main deformation front (Lewis, 1980). Offshore Kaikoura peninsula, another anticline (Lewis, 1980) is overlain by deeply-incised slope deposits. These anticlines attest for compression. Transpressional faults interpreted along the margin east of Cook Strait merge with the deformation front at the toe of the ridge indicating that some strike-slip motion is transferred southwestward along the margin. However, the intensity of the strike-slip motion must be small and seems to decrease southwestward because the canyons offshore Kaikoura peninsula are not laterally offset.

The lower slope terrace is 10–25 km wide, 1600–2200 m deep and is bounded to the southeast by the Hikurangi Channel (Figure 8). Seismic reflection data indicate that the terrace is underlain by at least 3000 m of stratified sediment. These sediments are trench fill turbidites overlain by slope deposits characterized by numerous imprints of channel beds filled up with sediments. The terrace sediments extend westward and are folded in the upper slope anticlines. These observations indicate that the segment of the southern Hikurangi margin located east of the shelf edge is a 15 km-wide, mainly compressive belt of deformation that includes trench-fill turbidites, young slope deposits and older rocks of the continental margin.

6. Discussion

6.1. The Pacific Plate and the Hikurangi Plateau

Faults induced by the flexure of the oceanic plate tend to parallel the trench or the seafloor fabric when the fabric trends less than 25°–30° from the trench direction (Masson, 1991). In the survey area, most normal faults trend 8–20° oblique to the trench and may reflect an oceanic fabric, but no fabric has been recognized on the Hikurangi Plateau or the adjacent oceanic crust. However, the normal faults parallel the N 5°–20° E structural directions of the Gisborne and Mahia seamounts supporting the inference that these faults are inherited structures reactivated by the bending of the plate.

The faulted topography of the western edge of the Hikurangi Plateau sharply contrasts with the smoothly bent oceanic crust immediately north of the Rapuhia Scarp (Figure 11). There is greater flexure of the oceanic crust north of the scarp than of the Hikurangi Plateau, indicating that the 15 km-thick plateau is more brittle and offers more resistance to bending than the oceanic crust. Such differential flexure should produce a tear fault along the Rapuhia Scarp as suggested by Davy (1992). Morphologic data indicate that about 30 km east of the trench, the split of the 1 km-high Rapuhia Scarp into three scarps correlates with a 400–650 m westward increase of the total height of the scarp at the trench axis. In addition to the high reflectivity of the scarps, strong reflectivity of the seafloor between the scarps suggest screes of coarse sediment related to active faulting (Figure 4). These correlations suggest that the Rapuhia Scarp segment close to the trench is the location of a down-dip tear fault resulting from the difference in slab pull between the dense oceanic crust to the north and the relatively more buoyant and less flexible crust of the Hikurangi Plateau to the south.

6.2. The upper plate

Oblique convergence along active margins commonly generates both trench-parallel and oblique structures, such as strike-slip faults (Fitch, 1972) that locally produce rotation of crustal blocks (Beck, 1983; Geist *et al.*, 1988; Ryan and Scholl, 1989; Lewis *et al.*, 1988; Lamb, 1988). The structural effects of the oblique convergence can, however, vary dramatically depending on the rate and obliquity of convergence, the nature and geometry of the upper and lower plates, the change in volume and physical properties of accreted material and the coupling between upper and lower plates (Ryan and Coleman, 1992; MacKay and Moore, 1990). In the following sections we discuss the development of strike-slip faults and block rotation in relation to the obliquity of the convergence and rock properties of the margin, and then we focus on the development of accreted ridges versus tectonic erosion.

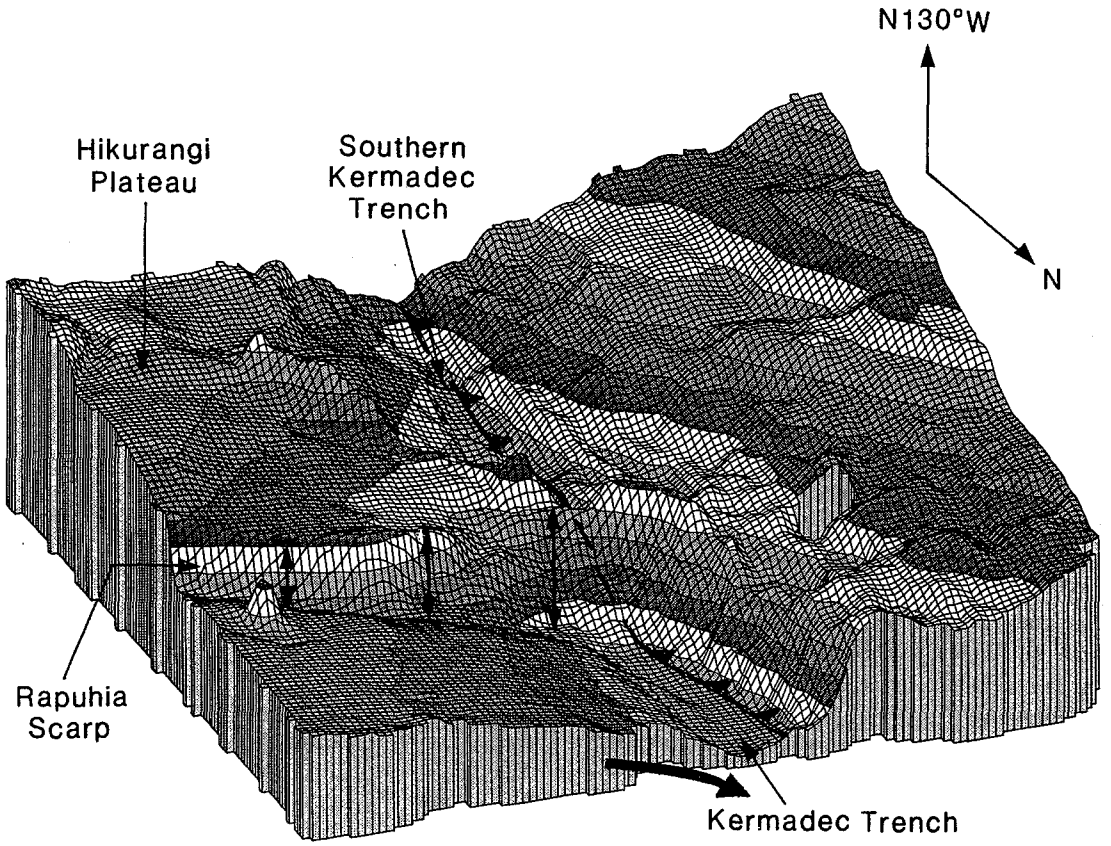

Fig. 11. 3D bathymetric diagram of the Kermadec subduction zone, where the Northern Hikurangi Plateau and the Rapuhia Scarp are being subducted; black line with teeth is the deformation front; note the difference in deformation style between the deep oceanic plate to the north and the Hikurangi Plateau to the south; vertical arrows show the increase in height of the Rapuhia Scarp toward the trench, suggesting that the scarp is activated as a tear fault when subducted.

6.2.1. Distribution of Strike-Slip Faulting and Crustal Block Rotation

Dextral strike-slip faulting is well documented onshore in the North Island forearc (Cashman *et al.*, 1992; Kelsey *et al.*, 1995; Van Dissen and Berryman, in press) and paleomagnetic studies (Wright and Walcott, 1986; Lamb, 1988; Mummy *et al.*, 1989; Walcott, 1989) indicate that the sites that were sampled in the forearc have undergone differential clockwise block rotations. Geophysical data presented above suggest that strike-slip faulting, as part of transpressive deformation, extends offshore along the active margin and that clockwise block rotation can be interpreted from the southern Kermadec margin.

Transpressional and strike-slip faults occur mainly in rocks located further up-slope than the fold and thrust belt of the accretionary wedge in the central Hikurangi margin. Along the southern Kermadec margin, however, strike-slip faults extend close to the deformation front, suggesting that the inter-plate coupling is strong enough to transfer some oblique motion through the upper plate. Alternatively, these strike-slip faults could have formed earlier, when the plate convergence was more oblique and the margin wider and thicker. An initially thicker lower margin can be inferred from its subsidence as indicated below. The large height (up to 1.2 km) and steepness (12°–17°) of the major N 35° E-trending scarp that divides the margin suggests that areas of the lower margin have strongly subsided relative to the upper one. Such a subsidence, which could result from tectonic erosion or lateral transport of rock slivers, could have lowered ancient strike-slip faults to near the trench. The strike-slip slivers that terminate near the trench could have been truncated by tectonic erosion.

Structures that appear to be rotated blocks are observed in the upper Kermadec margin, immediately north of the Ruatoria Scarp, where the subduction is moderately oblique. Assuming that the N 50° E-trending, southeastern boundary of each block was parallel

to the margin before rotation implies a c. 20° clockwise rotation around a vertical axis. Further south, near Cook Strait canyon, where trench-parallel motion predominates, block rotations are not inferred on the slope of the margin. However, deformed structural blocks, elongated parallel to the margin, are inferred to represent tectonic slivers transported southwestward along strike-slip faults. These observations support the model by Ryan and Coleman (1992) that suggests that moderately oblique subduction induces block rotation, whereas very oblique subduction generates strike-slip slivers and possibly block transport.

The obliquity of the convergence, which causes transpressional and strike-slip faulting, increases southward. This overall increase is, however, not uniform because the direction of individual segments of the margin varies significantly from N 28° E along the Southern Kermadec margin, through N 15° E at the northern Hikurangi margin, to N 50° E, N 70° E and N 45° E along the central and southern Hikurangi margins (Figure 12). Local change of the convergence obliquity does not necessarily imply change in strike-slip direction. For example, from 37° S to 40° S the obliquity of the convergence decreases by 10° but the direction of strike-slip faults relative to that of the plate convergence remains almost constant (Figure 12). This observation confirms that along the margin, strike-slip faulting is a large scale, primary feature with a regional cause, compared to indentation and collapse of the northern Hikurangi margin, which are secondary features superimposed on the margin, and have local causes.

The maximum strike-slip rate accommodated by the margin near latitude 41°30′ S can be estimated. Considering 4 cm/yr of convergence along N 262° E between the PAC and AUS plates (De Mets *et al.*, 1990) and a cumulative slip-rate of 1.8 to 2.5 cm/yr along N 40° E for the five active right lateral strike-slip faults of southern North Island (Van Dissen and Berryman, in press), a maximum of 0.5 to 1.2 cm/yr of strike-slip rate can be expected along faults located between the easternmost of these active faults (Wairarapa fault) and the deformation front (Figure 12).

6.2.2. Tectonic Accretion and Tectonic Erosion

The structural development of the accretionary wedge appears to be mainly controlled by turbidite distribution along the trench, the orientation of the continental margin with respect to the plate motion vector, and the number and size of seamounts on the downgoing plate.

The distribution of turbidites along the Hikurangi Trough and Kermadec Trench is irregular. Turbidites derived from the South Island are transported northward along the Hikurangi Trough (Lewis, 1994). Their thickest accumulation (3–4 km, Cole and Lewis, 1981) appears to be on the downwarped segment of crust of the Chatham Rise and Hikurangi Plateau, south of Cook Strait canyon. However, despite this great turbidite accumulation, the 30° angle between the margin and the plate convergence direction, and the minimum of 200–300 km of subduction that has occurred beneath the northern South Island (Reyners, 1989; Anderson and Webb, 1994), a large accretionary wedge of offscraped trench turbidites has not developed at the southern Hikurangi margin. Instead, a narrow transpressive belt has formed between the shelf edge and the deformation front suggesting that the plate convergence motion is dominantly accommodated further landward in the transpressive Kaikoura ranges, where the late Quaternary uplift rate is in the order of 1–10 mm/yr (Lamb and Bibby, 1989). Triangulation surveys have shown that the rate of motion across the northern South Island for the last 100 yr account for all the relative PAC-AUS plate motion, indicating that the interplate décollement has been locked over the last 100 yr (Walcott, 1978b; Bibby, 1981). The absence of a large accretionary wedge eastward of the Kaikoura ranges supports this result and indicate that the interplate décollement may have been locked during the deposition of the trench-fill turbidites.

The Plio-Pleistocene accretionary wedge has developed along the central Hikurangi margin (Figure 12), where the Hikurangi Trough contains 2–4 km of trench-fill turbidites (Lewis and Pettinga, 1993). This wedge, however, did not develop well immediately east of Cook Strait because of the highly oblique plate convergence. The landward boundary of the wedge has been refined using both seismic reflection and bathymetric data. In the southern half of the wedge, this boundary could be marked by a dextral strike-slip fault located immediately landward of the upper accreted ridge. In the northern half, the boundary is marked by the steep eastern edge of the upper margin transpressive strips.

Structures observed along the central Hikurangi margin support some strain partitioning. In the southern half of the wedge, strain partitioning is indicated by the strong obliquity (20°–30°) of the accreted ridges to the plate convergence direction, combined with evidence in the upper margin for transpressional and strike-slip faults sub-parallel to the accreted ridges. Accreted ridges appear to accommodate most of the orthogonal component of the convergence, whereas the upper margin and onshore

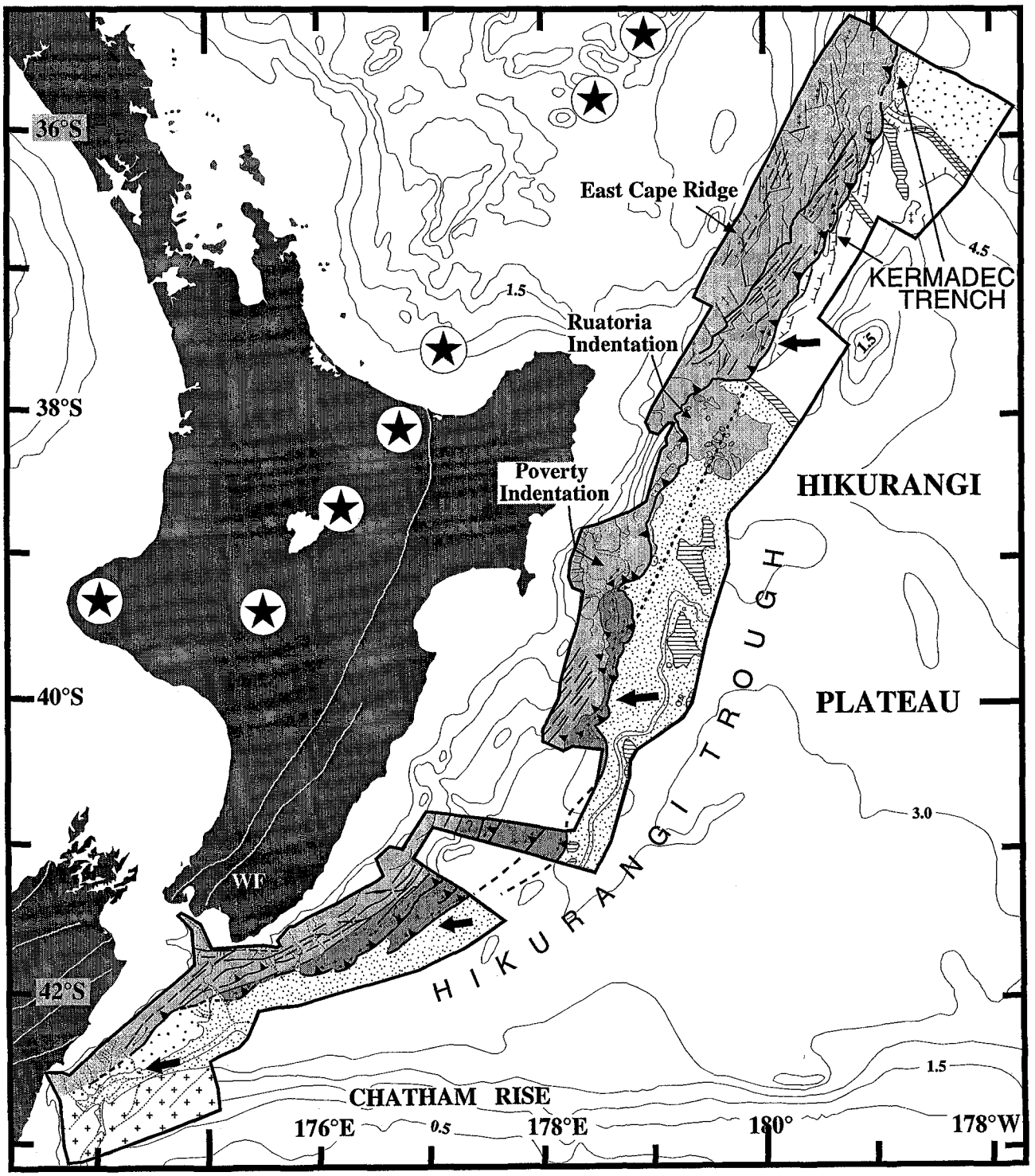

Fig. 12. Simplified structural map of the southern Kermadec and Hikurangi margin; 500 m contours; WF is Wairarapa Fault; dotted line is inferred location of the deformation front before the Northern Hikurangi margin was eroded. Other symbols as in Figures 5 and 8.

take up most of the strike-slip component. Strain partitioning is also evident in the margin near 40° S (Figure 12). At this location, accreted ridges trend sub-perpendicular to the convergence vector but strike-slip features of the upper margin trend 45° to the convergence vector.

No structural evidence for Plio-Pleistocene turbidite accretion was recognized along the re-entrant between the Ruatoria and Poverty indentations, although 1–1.5 km of turbidite trench fill exists along this segment of margin. The lower margin is dominated by gravitational collapse and we infer that this margin has been heavily eroded by seamount collisions. Some material detached from the margin has been transported downslope by block sliding as suggested by the Ruatoria Knolls. In addition, poorly reflective layers in trench fill along parts of the northern Hikurangi margin (Figure 6) suggest that local avalanche deposits supplement the well-stratified trenchfill turbidites. We relate the avalanche deposits to collapse of the margin. As indicated by the steepness (10°) of the margin and the juvenile aspect of the collapse within the Ruatoria indentation, we think that tectonic erosion is still actively preventing frontal tectonic accretion.

Little or no tectonic accretion is observed along the southern Kermadec Trench because the trench is devoid of turbidites and the pelagic sediments of the Hikurangi Plateau are generally subducted. Turbidites transported from the south appear to be partially diverted eastward by the Hikurangi Channel near the Mahia Seamount (Lewis, 1994) and partially trapped immediately north of the Ruatoria knolls by the knolls and ridge R3 (Figure 5). South of the Rapuhia Scarp, the southern Kermadec margin appears to be mainly controlled by tectonic erosion. North of the Rapuhia Scarp, the southward sweep of the scarp along the trench hampers tectonic accretion of some 250 m of turbidite trench-fill, and tectonically erodes the toe of the margin, generating a 15 km-arcward retreat of the deformation front.

7. Conclusions

We conclude that oblique subduction of the Hikurangi Plateau, which has areas of abundant seamounts and sediment-filled troughs, results in the following processes:

1. Pronounced transpressive deformation occurs offshore along most of the southern Kermadec-Hikurangi margin, including transpressional and strike-slip faults, apparent block rotations and possible lateral transport of blocks. Although the age of the faults with a significant strike-slip component is not known, they could have been initiated in the Miocene, when the plate convergence was more oblique.
2. Robust tectonic erosion controls the structural development of the northern Hikurangi margin and southern Kermadec margin. Tectonic erosion, favored by the lack of voluminous trench-fill turbidites, appears to result from a combination of strike-slip faulting that weakens the margin, and seamount and scarp collisions with the margin that trigger compressional faulting, followed by extensional faulting, slump and collapse.
3. Tectonic accretion of the Hikurangi wedge benefits from the great thickness of trench-fill turbidites adjacent to the deformation front and the small number and size of seamounts being subducted at this front. The wedge development is, however, impeded to the south by the increasing obliquity of convergence.
4. Compression dominates the structures of the narrow southern Hikurangi continental margin slope, where the interplate décollement appears to be locked.

The characteristic feature of this margin is the great structural variation caused by regional and local effects over short (200–300 km) distances.

Acknowledgements

We thank ORSTOM, INSU, Foundation for Research, Sciences & Technology of New Zealand, IGNS, NIWA and the Ministry of French Foreign Affairs for funding and supporting this collaborative work, IFREMER for providing R/V *l'Atalante* ship time and equipment, and GENAVIR officers, technicians and crew. We would like to thank P. J. Coleman, D. W. Scholl and R. Wood for suggestions and critical reviews to improve this manuscript.

References

Anderson, H. and Webb, T., 1994, New Zealand Seismicity: Patterns Revealed by the Upgraded National Seismograph Network, *N.Z. J. Geol. Geophys.* **37**, 477–493.

Ballance, P. F., 1976, Evolution of the Upper Cenozoic Magmatic Arc and Plate Boundary in Northern New Zealand, *Earth Planet. Sci. Lett.* **28**, 356–370.

Ballance, P. F., 1993, The New Zealand Neogene Forearc Basins, in Ballance, P. F. (ed.), *South Pacific Sedimentary Basins*, Hsü, K. J. (ser. ed.), Sedimentary Basins of the World, 2, Elsevier Sciences Publishers, Amsterdam, 177–193.

Barnes, P. M., 1994, Pliocene-Pleistocene Depositional Units on the Continental Slope off Central New Zealand: Control by Slope Currents and Global Climate Cycles, *Mari. Geol.* **117**, 155–175.

Beck, M. E., 1983, On the Mechanism of Tectonic Transport in Zones of Oblique Subduction, *Tectonophysics* **93**, 1–11.

Berryman, K. and Beanland, S., 1988, Ongoing Deformation of New Zealand: Rates of Tectonic Movement from Geological Evidence, *Transactions, the Institution of Professional Engineers New Zealand* **15**, 25–34.

Berryman, K. R., Beanland, S., Cooper, A. F., Cutten, H. N., Noris, R. J. and Wood, P. R., 1992, The Alpine Fault, New Zealand: Variation in Quaternary Structural Style and Geomorphic Expression, *Annales Tectonicâ* **VI**, 126–163.

Bibby, H. M., 1981, Geodetically Determined Strain across the Southern End of the Tonga–Kermadec Subduction Zone, *Geophysical Journal of the Royal Astronomical Society,* **66**, 513–533.

Carter, L. and McCave, I. N., 1994, Development of Sediment Drifts Approaching an Active Plate Boundary under the SW Pacific Deep Western Boundary Current, *Paleoceanography* **9**, 1061–1085.

Cashman, S. and Kelsey, H., 1990, Forearc Uplift and Extension, Southern Hawke's Bay, New Zealand: Mid-Pleistocene to Present, *Tectonics* **9**, 23–24.

Cashman, S. M., Kelsey, H. M., Erdman, C. F., Cutten, H. N. C. and Berryman, K., 1992, Strain Partitioning Between Structural Domains in the Forearc of the Hikurangi Subduction Zone, New Zealand, *Tectonics* **11**, 242–257.

Chanier, F. and Ferrière, J., 1991, From a Passive to an Active Margin: Tectonic and Sedimentary Processes Linked to the Birth of an Accretionary Prism (Hikurangi Margin, New Zealand), *Bulletin de la Société Géologique de France* **162**, 649–660.

Cole, J. W., 1990, Structural Control and Origin of Volcanism in the Taupo Volcanic Zone, New Zealand, *Bulletin of Volcanology* **52**, 445–459.

Cole, J. W. and Lewis, K. B., 1981, Evolution of the Taupo-Hikurangi Subduction System, *Tectonophysics* **72**, 1–21.

Collot, J. -Y., Delteil, J., Herzer, R., Wood, R., Lewis, K. B. and Shipboard Party, 1995, Sonic Imaging Reveals New Plate Boundary Structures Offshore New Zealand, *EOS Trans. Amer. Geophys. Union* **76**, 1–5.

Davey, F. J., Hampton, M., Childs, J., Fisher, M. A., Lewis, K. B. and Pettinga, J. R., 1986, Structure of a Growing Accretionary Prism, Hikurangi Margin, New Zealand, *Geology* **14**, 663–666.

Davy, B., 1992, The Influence of Subducting Plate Buoyancy on Subduction of the Hikurangi-Chatham Plateau beneath North Island, New Zealand, in Watkins, J. S., Zhiqiang, F. and McMillen, K. J. (eds.), *Geology and Geophysics of Continental Margins* **53**, The American Association of Petroleum Geologists, Tulsa, Ok., 75–91.

Davy, B. and Wood, R., 1994, Gravity and Magnetic Modelling of the Hikurangi Plateau, *Mari. Geol.* **118**, 139–151.

De Mets, C., Gordon, R. G., Argus, D. F. and Stein, S., 1990, Current Plate Motions, *Geophys. J. Int.* **101**, 425–478.

Delteil, J., Morgans, H. E. G. Raine, J. I., Field, B. D. and Cutten, H. N., Early Miocene Thin-skinned Tectonics Prior to Wrench Faulting in the Pongaroa District, Hikurangi Margin, North Island, New Zealand, *N.Z. J. Geol. Geophys.*, in press.

Fitch, T. J., 1972, Plate Convergence, Transcurrent Faults, and Internal Deformation Adjacent to Southeast Asia and the Western Pacific, *J. Geophys. Res.* **77**, 4432–4460.

Geist, E. L., Childs, J. R. and Scholl, D. W., 1988, The Origin of Summit Basins of the Aleutian Ridge: Implication for Block Rotation of an Arc Massif, *Tectonics* **7**, 327–341.

Gillies, P. N. and Davey., F. J., 1986, Seismic Reflection and Refraction Studies of the Raukumara Forearc Basin, New Zealand, *N.Z. J. Geol. Geophys.* **29**, 391–403.

Herzer, R. H., 1995, Seismic Stratigraphy of a Buried Volcanic Arc, Northland, New Zealand, and Implications for Neogene Subduction, *Marine & Petroleum Geology,* **12**, 5, 511–531.

Houtz, R. E., Ewing, J., Ewing, M. and Leonardi, A. G., 1967, Seismic Reflection Profile of the New Zealand Plateau, *J. Geophys. Res.* **72**, 4713-4729.

Kamp, P. J. J., 1984, Neogene and Quaternary Extent and Geometry of the Subducted Pacific Plate beneath North Island, New Zealand: Implications for Kaikoura Tectonics, *Tectonophysics* **108**, 241–266.

Karig, D. E., 1970, Ridges and Basins of the Tong-Kermadec Island Arc System, *J. Geophys. Res.* **75**, 239–254.

Katz, H. R., 1974, Margins of the Southwest Pacific, in Burk, C. A. and Drake, C. L. (eds.), *The Geology of Continental Margins,* Springer-Verlag, New York, 549–565.

Katz, H. R., 1982, Plate Margin Transition from Oceanic Arc-trench to Continental System: the Kermadec-New Zealand Example, *Tectonophysics* **87**, 49–64.

Katz, H. R. and Wood, R. A., 1980, Submerged Margin East of the North Island New Zealand, and its Petroleum Potential, in Luke, I. J. (ed.), *Symposium on Petroleum Potential in Island Arc, Small Ocean Basin, Submerged Margin and Related Areas.* **3**, 221–235.

Kelsey, H. M., Cashman, S. M., Beanland, S. and Berryman, K. R., 1995, Structural Evolution along the Inner Forearc of the Obliquely Convergent Hikurangi Margin, New Zealand, *Tectonics* **14**, 1–10.

Lamarche, G., Beanland, S. and Ravens, J. M., 1995, Deformation Style and History in the Eketahuna Region, Hikurangi Forearc, New Zealand, from Seismic Reflection data, *N. Z. J. Geol. Geophys.* **38**, 105–115.

Lamb, S. H., 1988, Tectonic Rotations about Vertical Axes during the last 4 M in part of the New Zealand Plate-Boundary Zone, *J. Struct. Geol.* **10**, 875–893.

Lamb, S. H. and Bibby, H. M., 1989, The last 25 Ma of Rotational Deformation in Part of the New Zealand Plate-Boundary Zone, *J. Struct. Geol.* **11**, 473–492.

Lewis, K. B., 1980, Quaternary Sedimentation of the Hikurangi Oblique-subduction and Transform Margin, New Zealand, *Spec. Publ. Int. Assoc. Sedimentol.* **4**, 171–189.

Lewis, K. B., 1994, The 1500-km-long Hikurangi Channel: Trench-axis Channel that Escapes its Trench, Crosses a Plateau, and Feeds a Fan Drift, *Geo-Mar. Lett.* **14**, 19–28.

Lewis, K. B. and Bennett, D. J., 1985, Structural Patterns on the Hikurangi Margin: An Interpretation of New Seismic Data, in Lewis, K.B. (ed.), *New Seismic Profiles, Cores and Dated Rocks from the Hikurangi Margin, New Zealand*, Oceanographic Field report, N. Z. Oceanographic Institute, 3–25.

Lewis, K. B. and Pettinga, J. R., 1993, The Emerging, Imbricate Frontal Wedge of the Hikurangi Margin, in Ballance, P. F. (ed.), *Basins of the Southwest Pacific. Sedimentary Basins of the World,* **2**, Elsevier Sciences Publishers, Amsterdam, 225–250.

Lewis, S. D., Ladd, J. W. and Bruns, T. R., 1988, Structural Development of an Accretionary Prism by Thrust and Strike-Slip Faulting: Shumagin Region, Aleutian Trench, *Bull. Geol. Soc. Am.* **100**, 767–782.

MacKay, M. E. and Moore, G. F., 1990, Variation in Deformation of the South Panama Accretionary Prism: Response to Oblique Subduction and Trench Sediment Variation, *Tectonics* **9**, 683–698.

Masson, D. G., 1991, Fault Patterns at Outer Trench Walls, *Mar. Geophys. Res.* **13**, 209–225.

Mortimer, N. and Parkinson, D. L., 1996, Hikurangi Plateau: A Cretaceous Large Igneous Province in the Southwest Pacific Ocean, *J. Geophys. Res.*, **101**, B1, 687–696.

Mummy, T. C., Lamb, S. H. and Walcott, R. I., 1989, The Raukumara Paleomagnetic Domain: Constraints on the Tectonic Rotation of the East Coast, North Island, New Zealand, from Paleomagnetic Data, *N.Z. J. Geol. Geophys.* **32**, 317–326.

Neef, G., 1984, Late Cenozoic and Early Quaternary Stratigraphy of the Eketahuna District (N153), *Bulletin of New Zealand Geological Survey* **96**.

Pettinga, J. R., 1982, Upper Cenozoic Structural History, Coastal Southern Hawke Bay, New Zealand., *N. Z. J. Geol. Geophys.* **25**, 149–191.

Pillans, B., 1986, A Late Quaternary Uplift Map for North Island, New Zealand, *Roy. Soc. N. Z. Bull.* **24**, 409–417.

Reyners, M., 1983, Lateral Segmentation of the Subducted Plate at the Hikurangi Margin, New Zealand: Seismological Evidence, *Tectonophysics* **96**, 203–223.

Reyners, M., 1989, New Zealand Seismicity 1964-87: An Interpretation, *N. Z. J. Geol. Geophys.* **32**, 307–315.

Ryan, H. F. and Coleman, P. J., 1992, Composite Transform-Convergent Plate Boundaries: Description and Discussion, *Mar. Petr. Geol.* **9**, 89–97.

Ryan, H. F. and Scholl, D. W., 1989, The Evolution of the Forearc Structures Along an Oblique Convergent Margin, Central Aleutian Arc, *Tectonics* **8**, 497–516.

Smith, E. G. C., Stern, T. A. and Reyners, M., 1989, Subduction and Back-Arc Activity at the Hikurangi Convergent Margin, New Zealand, *Pageoph* **129**, 203–231.

Spörli, K. B. and Ballance, P. F., 1989, Mesozoic Ocean Floor/Continent Interaction and Terrane Configuration, Southwest Pacific area around New Zealand, in Avraham, Z. B. (ed.), *The Evolution of the Pacific Ocean Margins* **9**, Oxford University Press, Oxford, 176–190.

Strong, C. P., 1994, Late Cretaceous Foraminifera from Hikurangi Plateau, New Zealand, *Mar. Geol.* **119**, 1–5.

Sutherland, R., 1995, The Australia-Pacific Boundary and Cenozoic Plate Motions in the Southwest Pacific: Some Constraints from Geosat data, *Tectonics*, **14**, 819–831.

Van der Lingen, G. J. and Pettinga, J. R., 1980, The Makara Basin: A Miocene Slope-basin along the New Zealand Sector of the Australian-Pacific Oblique Convergent Plate Boundary, in Ballance, P. F. and Reading, H. G. (eds.), *Sedimentation in Oblique-slip Mobile Zones*, **4**, International Association of Sedimentologists, 191–215.

Van der Lingen, G. J., 1982, Development of the North Island Subduction System, New Zealand, in Leggett, J. K. (ed.), *Trench-Forearc Geology*, **1**, The Geological Society of London, Blackwell Scientific Publications, London, 259–272.

Van Dissen, R. J. and Berryman, K.R., 1996, Surface-Rupture Earthquakes over the Last ca, 1000 years in the Wellington Region, New Zealand, and Implications for Ground Shaking Hazard, *J. Geophys. Res.*, in press.

Walcott, R. I., 1978a, Present Tectonics and Late Cenozoic Evolution of New Zealand, *Geophys. J. R. Astron. Soc.* **83**, 4419–4429.

Walcott, R. I., 1978b, Geodetic Strains and Large Earthquakes in the Axial Tectonic Belt of North Island, New Zealand, *J. Geophys. Res.* **83**, 4419–4429.

Walcott, R. I., 1989, Paleomagnetically Observed Rotations along the Hikurangi Margin of New Zealand, in Kissel, C. and Laj, C. (eds.), *Paleomagnetic Rotations and continental deformation*, Kluwer Academic Publisher, 459–471.

Wellman, H. W., 1953, Data for the Study of Recent and Late Pleistocene Faulting in the South Island of New Zealand, *N. Z. J. Sc. Technol* **B34**, 270–288.

Wood, R. and Davy., B., 1994, The Hikurangi Plateau, *Mar. Geol.*, 153–173.

Wright, I. C., 1993, Pre-shaped Rifting and Heterogeneous Volcanism in the Southern Havre Through Back-Arc Basin, *Mar. Geol.* **113**, 179–200.

Wright, I. C., 1994, Nature and Tectonic Setting of the Southern Kermadec Submarine Arc Volcanoes: An Overview, *Mar. Geol.* **118**, 217–236.

Wright, I. C. and Walcott, R. I., 1986, Large Tectonic Rotation of Part of New Zealand in the Last 5 Ma., *Earth Planet. Sci. Lett.* **80**, 348–352.